USGS-OFR-90-474

UNITED STATES DEPARTMENT OF THE INTERIOR

GEOLOGICAL SURVEY

RESULTS OF ROCK PROPERTY MEASUREMENTS MADE ON CORE SAMPLES FROM YUCCA MOUNTAIN BOREHOLES, NEVADA TEST SITE, NEVADA.
PART 1. BOREHOLES UE25A-4, -5, -6, AND -7.
PART 2. BOREHOLE UE25P#1.

By

Lennart A. Anderson

Open File Report 90-474

Prepared in cooperation with the U.S. Department of Energy

(Interagency Agreement DE-AI08-78ET44802)

Denver, Colorado
1991

Copies of this Open-File Report
may be purchased from

Books and Open-File Reports Section
Branch of Distribution
U.S. Geological Survey
Box 25425 Federal Center
Denver, Colorado 80225

PREPAYMENT IS REQUIRED

Price information will be published
in the monthly listing
"New Publications of the Geological Survey"

FOR ADDITIONAL ODERING INFORMATION

CALL: Commercial: (303) 236-7476
FTS: 776-7476

USGS-OFR-90-474

UNITED STATES DEPARTMENT OF THE INTERIOR

GEOLOGICAL SURVEY

Results of rock property measurements made on core samples from Yucca Mountain boreholes, Nevada Test Site, Nevada. Part 1. Boreholes UE25A-4, -5, -6, AND -7. Part 2. Borehole UE25P#1.

By

Lennart A. Anderson

Open-File Report 90-474

Contents

Results of rock property measurements made on core samples from Yucca Mountain boreholes, Nevada Test Site, Nevada. Part 1. Boreholes UE25a-4, -5, -6, and -7. Part 2. Borehole UE25p#1.

by

Lennart A. Anderson

ABSTRACT

Laboratory measurements of resistivity, bulk and grain density, porosity, compressional sonic velocity, water permeability, magnetic susceptibility, and remanent magnetization were made on core samples from the Yucca Mountain UE25a-4,-5,-6 and -7 boreholes located in Drill Hole Wash at the Nevada Test Site. The samples are representative of lithologic variations to be found in the Tiva Canyon, Yucca Mountain, Pah Canyon, and the upper Topopah Spring Members of the Paintbrush Tuff. Boreholes penetrated to a depth of appproximately 152 meters (500 ft.). The Paintbrush Tuff consists primarily of nonwelded to densely welded rhyolitic ash-flow tuff with relatively thin beds of ash-fall tuff typically separating each Member.

Resistivity and bulk density measurements were made on samples containing natural pore waters and repeated following resaturation with local tap water. Density comparisons indicate the samples to be undersaturated in their natural environment as expected in that the boreholes did not intersect the water table. However, the resistivity values in both saturation modes are very nearly the same in most samples suggesting a sufficient volume of pore water exists in the in-place rock to provide continuous conduction paths through the sample.

The nonwelded tuff can be recognized by its high porosity, low resistivity, and low sonic velocity relative to those rock property values found in the densely welded tuff generally confined to the Topopah Spring Member. Bulk and grain densities are lower in the nonwelded tuffs as a result of clay alteration. Water permeability is highly variable controlled primarily by pore structure rather than by the porosity of the rock.

Core was also obtained from borehole UE25p#1 located approximately 3 km east of Yucca Mountain. Most samples are from the the Paleozoic Lone Mountain Dolomite formation underlying the Yucca Mountain tuffs. The grain density of the dolomite is uniformly 2.86 Mg/m^3 but bulk density variations exist because of porosity variations. Resistivity also varies with porosity ranging from 300 to 6100 ohm-meters when containing the original pore waters. Porosities vary from 0.3 to 9.9 percent with water permeability values somewhat aligned with those of porosity. Sonic velocity exceeds 4 km/sec and the magnetic properties of the dolomite are very low relative to the overlying tuff series.

Part 1. Introduction

Forty-four core samples from the Yucca Mt. UE25a-4,-5,-6,and -7 boreholes on the Nevada Test Site (NTS) were obtained for selected rock property measurements as part of a study to determine the extent of lateral structural variations inferred from the interpretation of electrical surface and borehole surveys (Senterfit and Others, 1982; Daniels and Others, 1981). The site, informally known as Drill Hole Wash, is a linear, northwest oriented dry stream bed crossing the eastern boundary of Yucca Mountain. Yucca Mountain, currently under evaluation for its suitability as a potential repository for radioactive waste products, lies in the southwest sector of NTS within the Topopah Spring SW Quadrangle (figure 1). The boreholes, enclosed within a triangular area of about 0.09 square kilometers, were drilled to a depth of 152.4 meters (500 feet) except that UE25a-7 was inclined from the vertical by 26 degrees. As a result, the effective probing depth of the -7 borehole was approximately 137 meters (450 feet).

The core samples represent four members of the Paintbrush Tuff (Spengler and Rosenbaum, 1980). With increasing depth, the members are the lower section of the Tiva Canyon, Yucca Mountain, Pah Canyon, and the upper part of the Topopah Spring. The rocks, Miocene in age, are described as nonwelded to densely welded ash-flow and bedded tuffs.

Core samples were selected at the drill sites so as to be representative of the major lithologic variations observed within the named stratigraphic units. Each sample was wrapped in aluminum foil and encased in beeswax shortly after extraction from the drillholes. Upon delivery to the Denver Laboratories of the USGS, the samples were measured for electrical resistivity, porosity, bulk density, grain density by both helium and water invasion methods, compressional sonic velocity, magnetic susceptibility, remanent magnetization, and water permeability. The results of the measurements are intended for use in the interpretation of inhole and surface geophysical surveys as well as to provide a means for rock property characterization in that the section studied is above the static water level where many conventional geophysical borehole methods are ineffective.

Sample Measurement Procedures:

The manner with which the samples were prepared and measured for their various physical properties are generally the same as those used in the analysis of core samples from the Yucca Mountain UE25a-1 borehole (Anderson, 1981). A helium pycnometer was added for grain volume determinations, as described by Johnson, (1979), to possibly improve on the results obtained using the water invasion method.

Resistivity, bulk density, and compressional sonic velocity measurements were made initially on large volume core samples (250-450 cc) containing original pore waters. After drying and resaturation with local tap water (18-22 ohm-m), resistivity measurements were repeated and densities and porosity determined following a series of weighings in the dry, saturated, and suspended states. The samples were then reduced in size to a volume of about 12 cc for grain density determinations by helium pycnometry, and for magnetic intensity and water permeability measurements.

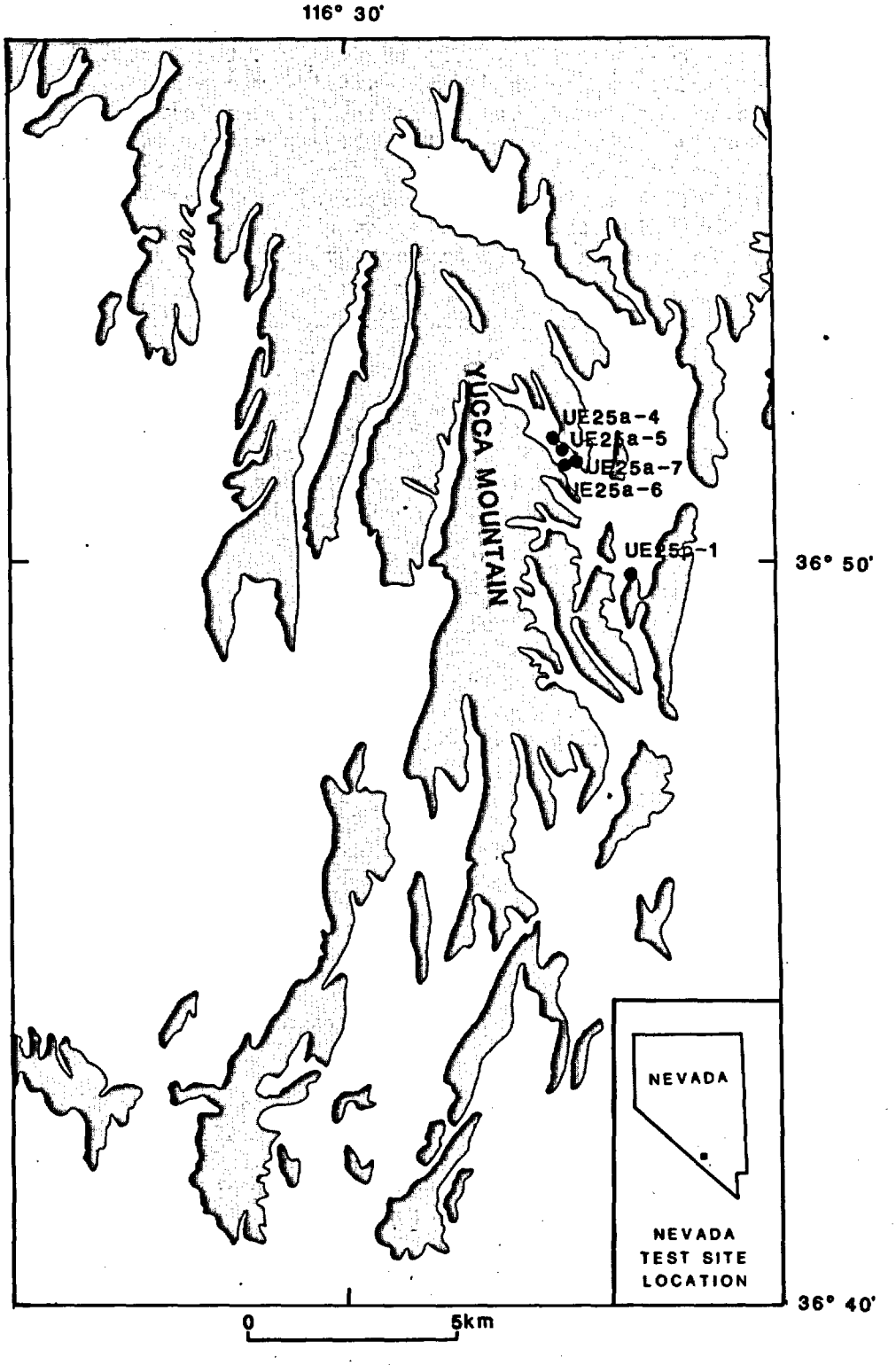

Figure 1. Map of the Nevada Test Site showing the locations of the Yucca Mountain UE25a-4, -5, -6, -7 and UE25p#1 boreholes.

The samples, as received, were cut to a cylindrical shape while still in their beeswax protective coverings. The beeswax was then removed, the samples surficially dried, and then measured for resistivity containing the in place pore waters. This measurement, loosely referred to as "natural-state" resistivity, was often the only one of this type possible on the poorly compacted, non-welded tuff samples. It was also of interest, however, to compare the natural state resistivities with resistivities made on the fully saturated rock to determine the continuity of the in situ pore waters as a possible mechanism for contaminant transport by diffusion processes.

Laboratory Measurement Procedures and Results

Density measurement results:

Calculated values of bulk density containing the natural pore waters, (NBD); saturated bulk density, (SBD); dry bulk density, (DBD); grain density, (GDA and GDH by water and helium invasion methods, respectively); and water-accessible porosity, (ϕ), for the total number of borehole samples were obtained as follows:

NBD = Wn/Vc, where Wn is the weight of the sample containing in-situ pore waters and Vc is the calipered volume of the sample.

SBD = Ws/Vb, where Ws is the weight of the saturated sample and Vb is the bulk volume of the sample as determined by a water displacement technique as described by Chleborad and others, (1975).

DBD = Wd/Vb, where Wd is the dry weight of the sample.

$\phi = (W_s - W_d)/V_b$ where ϕ is the fractional porosity of the sample.

GDA = DBD*ε/(1-ϕ), where ε is the density of distilled water at ambient temperature.

GDH = Wd/Vg, where Vg is the grain volume of the sample determined by helium pycnometery.

Water permeability was measured using cores 1 inch (25.4mm) in diameter and length. Held within a stainless steel flow cell distilled water was forced through the sample using a driving pressure of 50 psi and a confining pressure of approximately 100 psi. A capillary tube of known inside diameter was attached to the outflow side of the flow cell and flow rates through the sample were determined by measuring the time (t) required for the displacement of a fixed volume of water (V) within the capillary. Permeabilities (kd) were calculated from the equation

$$kd = \mu V l / t A \Delta P$$

where μ is the viscosity of the pore fluid in pascal-sec; ΔP is the net pressure difference across the length of the sample in pascals; and A and l are the cross-sectional area and length of the sample, respectively. Units of the permeability equation are in cm^2 but expressed in darcies by use of the conversion 1 darcy = $0.0981 * 10^{-8}$ cm^2 (Olsen and Daniel, 1981).

Compressional sonic velocity was determined using a pulse technique described by Obert and Duvall (1967). The sample was held between pressure plates at zero confining pressure, each plate containing a piezoelectric transducer made of barium titanate crystals used for energy conversion. A high voltage pulse converted to a compressional wave was propagated through the sample, detected and reconverted to a voltage pulse by the receiver crystal. Both transmitted and received pulses are displayed on an oscilloscope and the time separation recorded. Sonic velocity was calculated using the equation

$$Vp = 1/(t-td)$$

where 1 is sample length, t is pulse travel time, and td is system delay time.

The results of the density measurements are listed in Table 1.

Table 1. Calculated values of density obtained on UE25a-4,-5,-6,and -7 borehole samples. [NBD, natural bulk density using calipered volume; DBD, SBD, and GDA, dry bulk density, saturated bulk density, and grain density, respectively, using bulk and grain volume determined by the bouyancy method; GDH, grain density using grain volume determined by helium pycnometry on bulk samples]. The stratigraphic Member of the Paintbrush Tuff represented by the sample is also indicated. Leader (-) indicates sample not suitable for measurement.

Borehole UE25a-4

Sample Depth in meters (feet)	NBD	SBD	DBD	GDA	GDH	Stratigraphic Member
	----------		Mg/m^3	----------		
46.8 (153.5)	1.56	1.74	1.33	2.26	2.31	Yucca Mt.
92.9 (304.7)	1.59	-	-	-	2.39	Topopah Spring
102.8 (337.2)	2.37	2.42	2.35	2.53	2.50	"
111.6 (366.0)	2.13	2.22	2.03	2.51	2.51	"
120.0 (393.6)	2.35	2.41	2.30	2.60	2.60	"
127.3 (417.5)	2.22	2.35	2.21	2.57	2.57	"
136.3 (447.1)	2.30	2.35	2.22	2.56	2.55	"
143.3 (470.0)	2.27	2.35	2.22	2.55	2.55	"
150.1 (492.3)	2.34	2.41	2.31	2.56	2.56	"

Borehole UE25a-5

Sample Depth in meters (feet)	NBD	SBD	DBD	GDA	GDH	Stratigraphic Member
	----------		Mg/m^3	----------		
41.4 (135.8)	1.87	1.88	1.46	2.53	2.44	Tiva Canyon
51.6 (169.2)	1.73	-	-	-	2.34	Bedded Tuff
60.8 (199.4)	1.62	-	-	-	2.38	Pah Canyon
69.8 (228.9)	1.61	-	-	-	2.35	"

Borehole UE25a-5 (continued)

74.1 (243.0)	1.69	-	-	-	2.41	Topopah Spring
85.8 (281.4)	2.51	2.54	2.51	2.58	2.51	"
93.1 (305.4)	2.35	2.35	2.31	2.41	-	"
102.3 (335.5)	2.34	2.38	2.27	2.56	2.54	"
109.3 (358.5)	2.25	2.33	2.17	2.59	2.58	"
116.8 (383.1)	2.31	2.35	2.22	2.57	2.56	"
124.9 (409.7)	2.29	2.35	2.22	2.56	2.54	"
134.1 (439.8)	2.30	2.33	2.20	2.52	2.50	"
142.0 (465.8)	2.09	2.22	2.03	2.49	2.49	"
146.4 (480.2)	2.30	2.32	2.20	2.50	2.49	

Borehole UE25a-6

Sample Depth in meters (feet)	NBD	SBD	DBD	GDA	GDH	Stratigraphic Member
			Mg/m^3			
32.7 (107.3)	2.32	2.33	2.23	2.49	2.46	Tiva Canyon
39.3 (128.9)	1.97	1.99	1.70	2.39	2.44	"
48.2 (158.1)	1.57	-	-	-	2.34	Yucca Mt.
56.1 (184.0)	1.56	-	-	-	2.39	Bedded Tuff
94.9 (311.3)	2.30	2.35	2.20	2.59	2.60	Topopah Spring
104.9 (344.1)	2.25	2.32	2.16	2.57	2.57	"
112.4 (368.7)	2.29	2.36	2.23	2.56	2.56	"
121.0 (396.9)	2.25	2.32	2.18	2.54	2.52	"
132.9 (435.9)	2.24	2.29	2.14	2.50	2.51	"

Borehole UE25a-7

Sample Depth in meters (feet)	NBD	SBD	DBD	GDA	GDH	Stratigraphic Member
			Mg/m^3			
53.3 (174.8)	1.90	1.92	1.49	2.60	2.47	Tiva Canyon
59.6 (195.5)	1.53	1.65	1.09	2.46	2.34	Yucca Mt.
71.3 (233.9)	1.52	1.60	1.17	-	2.39	Pah Canyon
79.4 (260.4)	1.46	-	-	-	2.37	"
87.6 (287.3)	1.54	-	-	-	-	Topopah Spring
95.2 (312.3)	2.48	2.50	2.49	2.53	2.49	"
102.1 (334.9)	2.32	2.38	2.28	2.53	2.52	"
114.4 (375.2)	2.28	2.34	2.19	2.59	2.58	"
120.8 (396.2)	2.26	2.32	2.16	2.58	2.57	"
132.4 (434.3)	2.22	2.36	2.22	2.57	2.54	"
138.3 (453.6)	2.28	2.34	2.20	2.56	2.54	"
144.7 (474.6)	2.26	2.32	2.18	2.53	2.53	"

Based on the tabulated data the NBD values of the measured samples are less than the SBD values because of the undersaturated condition of the core as received. In some samples the NBD values approximate those of SBD while in others the NBD values are equal or nearly equal to DBD indicating a variability in the degree to which the rock is saturated. Variations in saturation levels above the water table are, conceivably, a naturally occurring phenomenon. However, there is always the concern that the time of exposure to the environment following core withdrawal from the borehole may

have contributed to the differing levels of dehydration. Consequently, the NBD values, plotted in figure 2 as continuous data sets because of their greater number of data points, are probably not always true indicators of the in situ bulk densities of the rock. However, the density characterization provided by the NBD plot is valid inasmuch as the offsets between the NBD and SBD data points are insignificant relative to the density variations between and within the lithologic Members.

By observation and correlation with the stratigraphic plots presented by Spengler and Rosenbaum, 1980, bulk density variations are an indicator of the degree to which the rock has been welded. The poorly consolidated samples from the Yucca Mt. and Pah Canyon Members and the intervening bedded tuffs produce the lowest density values matched in some instances by the non-welded tuffs in the upper zone of the Topopah Spring Member. Bulk densities of the Tiva Canyon show varying degrees of welding; the lowest values occurring near the base of the lithologic unit. The welded section of the Topopah Springs Member is reasonably uniform with only slight variations in density indicated.

According to Orkild (1965), the individual Members of the Paintbrush Tuff are petrographically similar, therefore the observed variations in grain density between samples must be caused by clay alteration, pumice content, and percentage of phenocrysts or lithic fragments found within the rock. Pumice, with its occluded porosity, tends to produce a lower than actual grain density when measurements are made on the rock in its bulk form.

Grain density, determined by both water and helium invasion methods, is plotted in figure 3. The GDH values, represented by a larger number of samples, are shown as an interconnected data set overlain by the GDA values. Grain densities determined by a series of weight measurements involving core samples in both wet and dry modes assumes that the pore spaces of the rock are totally filled with water. Total filling is not possible when the size of the connecting pore interstices is less than the diameter of a water molecule. The resulting uncertainty is largely overcome through the use of helium as the pore-filling medium because of its nonadsorbing qualities and its extremely small molecular diameter. Neither method will prove completely accurate if sealed pore spaces exist within the rock.

Normally, it may be expected that in fine-grained rocks, grain densities by helium pycnometry will be somewhat higher than those produced by water invasion. In this instance, however, a direct comparison of the grain density values obtained for each sample is not necessarily valid inasmuch as the sample volume used with the pycnometer was substantially less than the sample volume used in determining the grain density by water injection. Where comparisons can be made, discrepancies in grain density values are greatest within the Tiva Canyon, Yucca Mt., Pah Canyon, and Bedded Tuff samples. Grain densities determined by both methods are the same or nearly the same for each sample of welded tuff from the Topopah Spring Member. The close correspondence in the grain densities of the Topopah Spring samples attests to their mineralogical homogeneity and their relatively open pore structure.

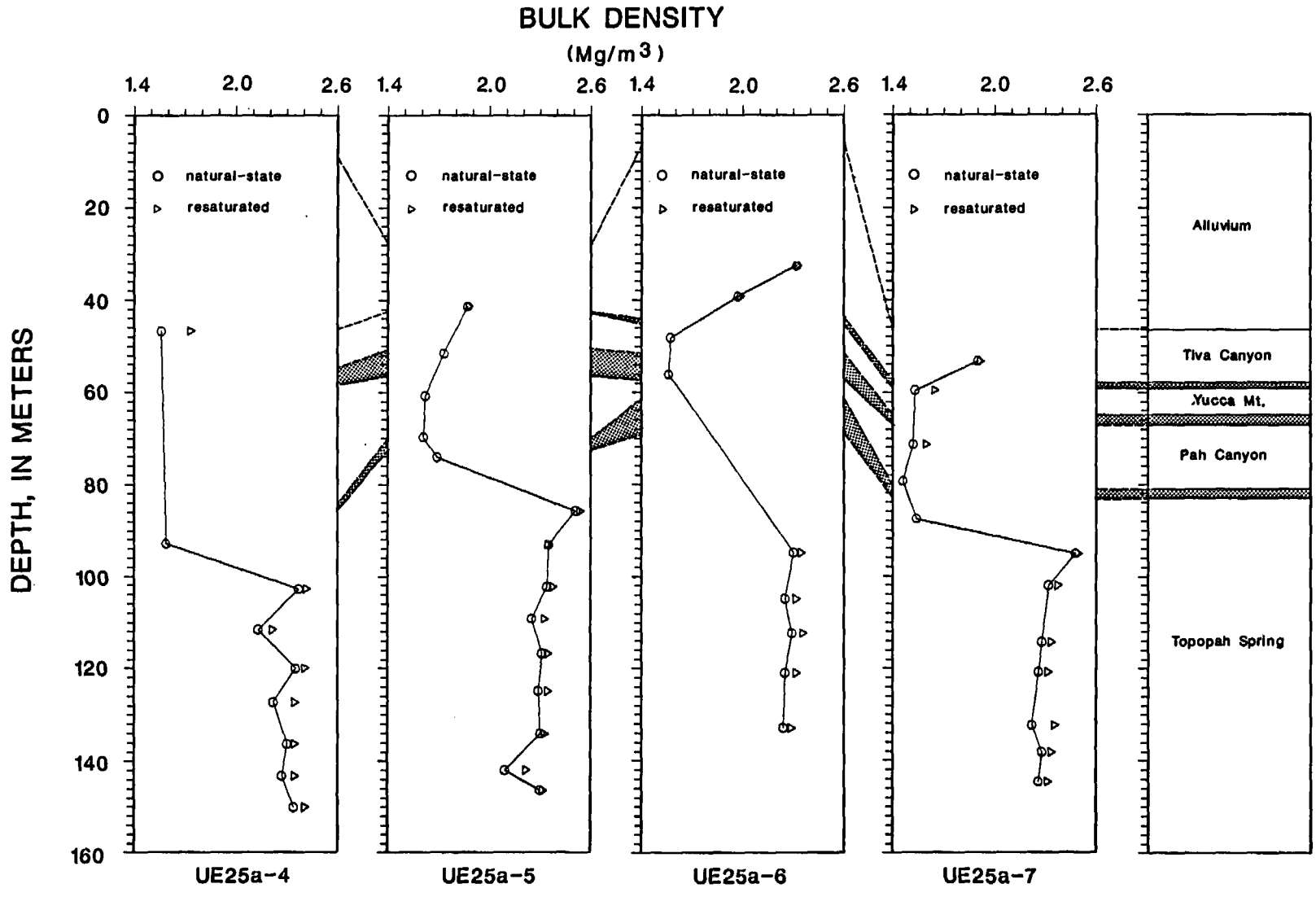

Figure 2. Plots of bulk density values measured on core samples obtained from the Yucca Mt. UE25a-4, -5 -6, and -7 boreholes. Circles designate those measurements made on samples containing in place or natural-state pore waters and the triangles designate measurements made following resaturation with local tap water. The stratigraphic section, as presented by Spengler and Rosenbaum, 1980, is shown on the right hand side of the figure with the bedded tuff intervals darkened to demonstrate continuity between boreholes.

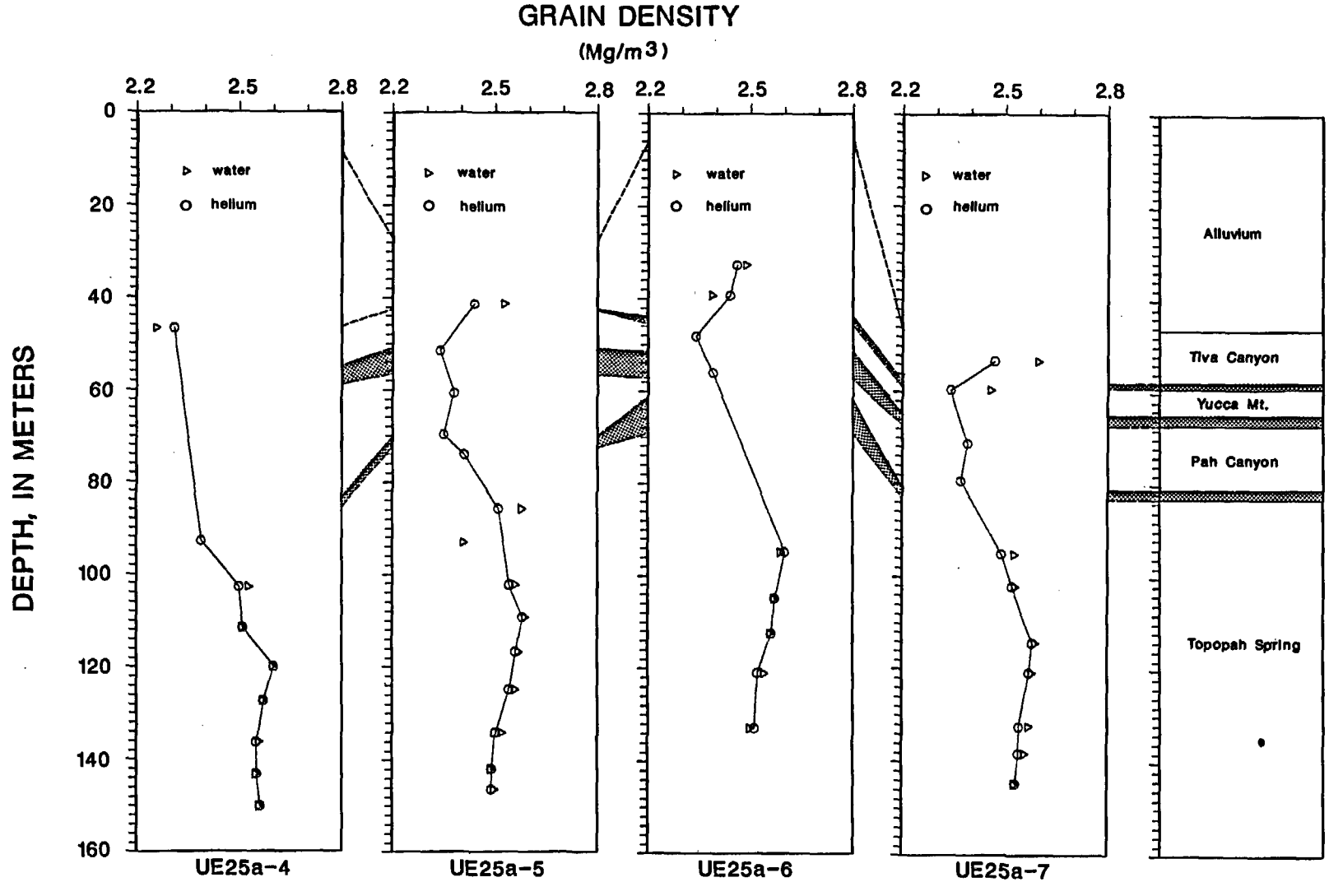

Figure 3. Plots of grain density values measured on core samples obtained from the Yucca Mt. UE25a-4, -5, -6 and -7 boreholes. Sample volume determinations were made using both helium and water invasion techniques.

Although the various members of the Paintbrush Tuff are closely related compositionally as verified by Spengler and Rosenbaum, 1980, an appreciable range of grain densities was found to exist in those core samples measured. As previously indicated, the variability in grain density may be caused by differences in pumice content between samples because of its occluded porosity and possibly because of the partial alteration of pumice to clay (Spengler and Rosenbaum, 1980). Phenocrysts of pyroxene and hornblende within the matrix of the rock, and calcite veinlets formed within fractures also act to alter the apparent grain densities of the tuffs. The grain density of pumice from three locations other than Yucca Mountain was determined to be in the range of 1.4 to 1.9 Mg/m^3 but their intrinsic grain density is 2.65 Mg/m^3 (Johnson, G.R., 1982, USGS, Personal Communication). Thus, it may be concluded that the low grain density samples contain a significant quantity of pumice whereas the high grain density samples bear a proportionately higher level of calcite and mafic minerals adding to the net grain density of the rock. The grain density of clays varies as a function of their state of hydration averaging about 2.5 Mg/m^3 which does not constitute a significant departure from that determined for the whole rock.

Results of porosity, permeability, and sonic velocity measurements:

Porosity values listed in Table 2 and plotted in figure 4 were made in conjunction with density determinations using the water invasion method. This measurement is an "effective" porosity from a hydrological viewpoint. The highest porosities measured are on those samples from the Yucca Mt. and Pah Canyon Members taken from the UE25a-7 borehole and on samples from the lower part of the Tiva Canyon Member. Based on their appearance and inability to withstand resaturation without crumbling, it is estimated that the porosity of those samples for which no measurement was possible is in the 30 to 50 percent range. The lowest porosities measured are associated with a quartz-latite caprock at the top of the welded section within the Topopah Spring Member. This section is represented in all but the UE25a-6 borehole samples. Below the caprock the welded tuffs have porosities in the range of approximately 10 to 20 percent averaging about 14 percent.

Table 2. Calculated values of porosity, compressional sonic velocity, and water permeability obtained on UE25a-4, -5, -6, and -7 borehole samples. Leader (-) indicates measurement not possible.

Borehole UE25a-4

Sample Depth in meters (feet)	Porosity in percent	Compressional Sonic Velocity in kilometers/second	Permeability in millidarcies
46.8 (153.5)	41.2	1.80	2480
92.9 (304.7)	-	-	-
102.8 (337.2)	7.1	4.42	0.52
111.6 (366.0)	19.1	3.96	38.8
120.0 (393.6)	11.6	4.62	0.475
127.3 (417.5)	14.1	3.38	1.05
136.3 (447.1)	13.4	4.06	0.795
143.3 (470.0)	12.9	3.68	0.61
150.1 (492.3)	9.9	4.04	0.015

Borehole UE25a-5

Sample Depth in meters (feet)	Porosity in percent	Compressional Sonic Velocity in kilometers/second	Permeability in millidarcies
41.4 (135.8)	42.2	2.59	310
51.6 (169.2)	-	0.93	-
60.8 (199.4)	-	0.81	-
69.8 (228.9)	-	-	-
74.1 (243.0)	-	1.03	-
85.8 (281.4)	2.9	5.24	0.015
93.1 (305.4)	4.2	4.59	0.575
102.3 (335.5)	11.4	4.42	0.175
109.3 (358.5)	16.2	4.06	0.045
116.8 (383.1)	13.6	4.21	0.11
124.9 (409.7)	13.2	4.25	0.325
134.1 (439.8)	12.8	4.19	0.058
142.0 (465.8)	18.4	3.98	0.05
146.4 (480.2)	12.1	4.19	0.795

Borehole UE25a-6

Sample Depth in meters (feet)	Porosity in percent	Compressional Sonic Velocity in kilometers/second	Permeability in millidarcies
32.7 (107.3)	10.5	4.21	0.051
39.3 (128.9)	28.9	3.22	0.077
48.2 (158.1)	-	2.46	4170
56.1 (184.0)	-	1.40	-
94.9 (311.3)	15.0	4.11	1.45
104.9 (344.1)	16.0	4.12	1.24
112.4 (368.7)	12.8	4.13	0.215
121.0 (396.9)	14.4	3.98	0.767
132.9 (435.9)	14.2	4.03	0.0009

Borehole UE25a-7

Sample Depth in meters (feet)	Porosity in percent	Compressional Sonic Velocity in kilometers/second	Permeability in millidarcies
53.5 (174.8)	42.8	2.19	1430
59.6 (195.5)	55.5	2.18	202
71.3 (233.9)	43.1	2.10	-
79.4 (260.4)	-	1.93	197
87.6 (287.3)	-	1.41	-
95.2 (312.3)	1.6	4.93	0.22
102.1 (334.9)	9.9	4.40	0.825
114.4 (375.2)	15.5	4.15	0.65
120.8 (396.2)	16.5	4.09	3.97
132.4 (434.3)	13.5	4.17	1.67
138.3 (453.6)	14.2	4.24	0.04
144.7 (474.6)	14.0	4.04	0.0009

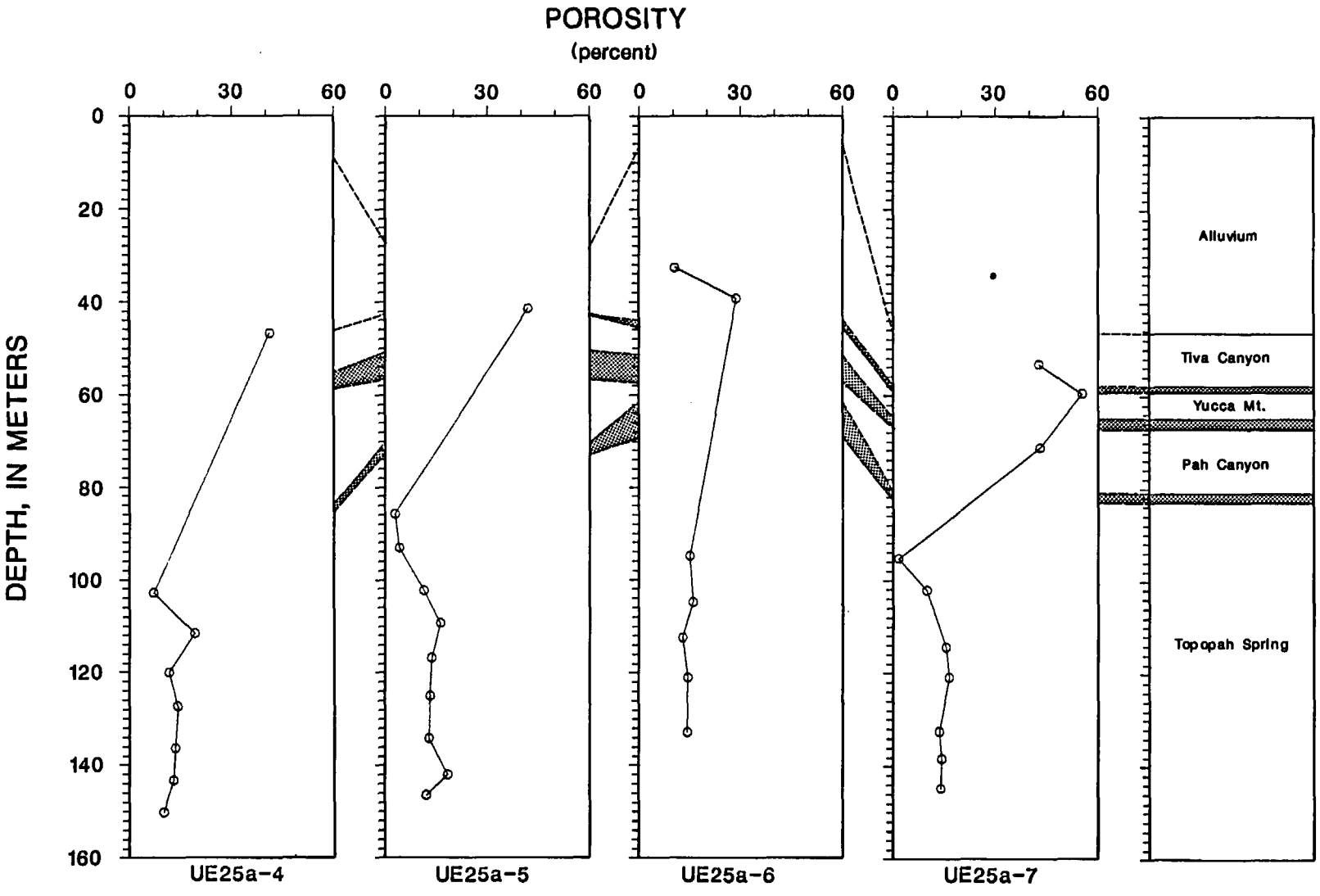

Figure 4. Porosity plots of sample data obtained on core from the Yucca Mt. UE25a-4, -5, -6, and -7 boreholes.

Water permeability in coarse-grained rock typically varies as a function of porosity provided that the rock is not fractured. In fine-grained rock such as densely welded tuff, there are wide departures from a systematic porosity/permeability relationship. The permeability values listed in Tables 2 and 5 are initial values. Repeat measurements made sequentially over a period of time show a general decrease in permeability values for virtually all samples of partially-to-densely welded tuff, varying from a few percent to as much as two orders of magnitude. Reversing flow direction reproduces the original value indicating the cause of the reduction in permeability values with time to be the result of the movement of unattached mineral grains within the pore spaces of the rock. Apparently, grain buildup causes clogging at the orifices of the interstitial pore spaces sufficient to severely limit fluid flow.

Figure 5 is a plot of the permeability data versus sample depth for the four boreholes. The highest values in units of millidarcies occur at the base of the Tiva Canyon, Yucca Mt., and Pah Canyon Members attesting to their high porosity and nonwelded condition. An exception exists in the -6 borehole where both Tiva Canyon samples are partially to moderately welded having nearly equal permeability values. Porosities of these samples, however, differ by a factor of almost 3 indicating the sample from the 39.3 meter depth to be less welded than the sample from the 32.7 meter depth. Possibly pore size dimensions within the two samples are equivalent thereby constituting the controlling element in limiting fluid flow through the rock. The permeabilities of the Tiva Canyon samples from the -6 borehole are often less than those of the moderately to densely welded samples from the Topopah Spring Member which also may be attributed to differences in pore size dimensions.

Despite the uniformity in porosity values within samples from the lower section of the Topopah Spring Member, permeabilities vary from less than a microdarcy to tens of millidarcies. Although an effort was made to avoid making measurements on core having obvious microfractures aligned parallel to the axis of the sample, it is likely that microfractures play a part in conducting fluid through the rock. As before, welding levels and their apparent tendency to reduce pore diameters are considered to be a major factor in controlling the permeability of the rock.

Because laboratory measurements of acoustic velocity were made on core in the absence of a confining pressure and the transmitted energy forced to follow a prescribed travel path, acoustic velocities are suspected to be slightly lower than those derived from borehole logs. The laboratory data is, however, useful in predicting the relative velocity response for the various tuff members in the in situ environment.

In a general sense, based on the acoustic velocity plots shown in figure 6, the measured velocities appear to be dependent upon the textural properties of the rock and the degree to which the tuffs have been welded. The lowest values, ranging from 0.81 to 1.03 kilometers/second, are found in the UE25a-5 borehole samples representing the Yucca Mountain, Pah Canyon, and upper

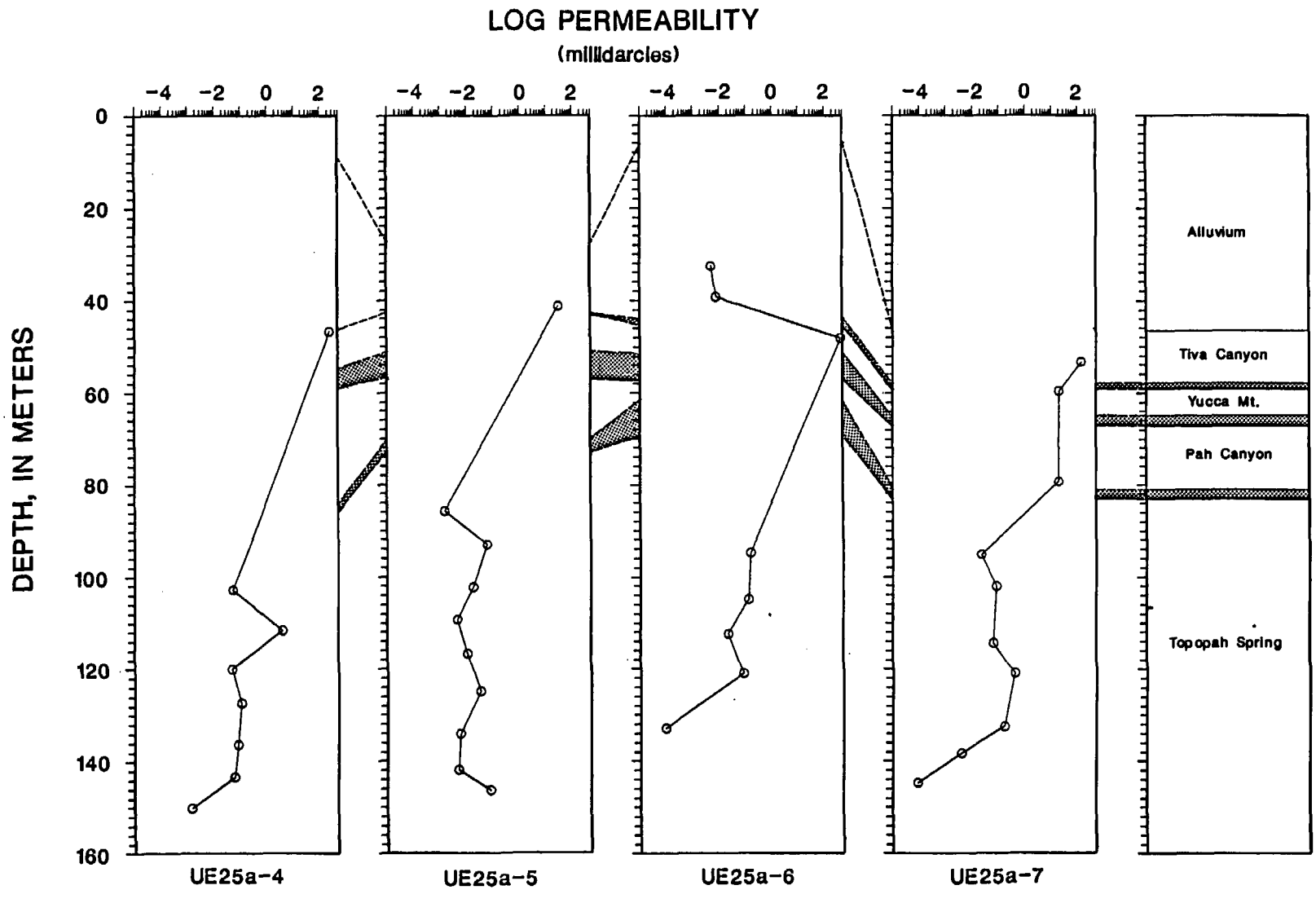

Figure 5. Plots of permeability or hydraulic conductivity values obtained on core samples from the Yucca Mountain UE25a-4, -5, -6, and -7 boreholes.

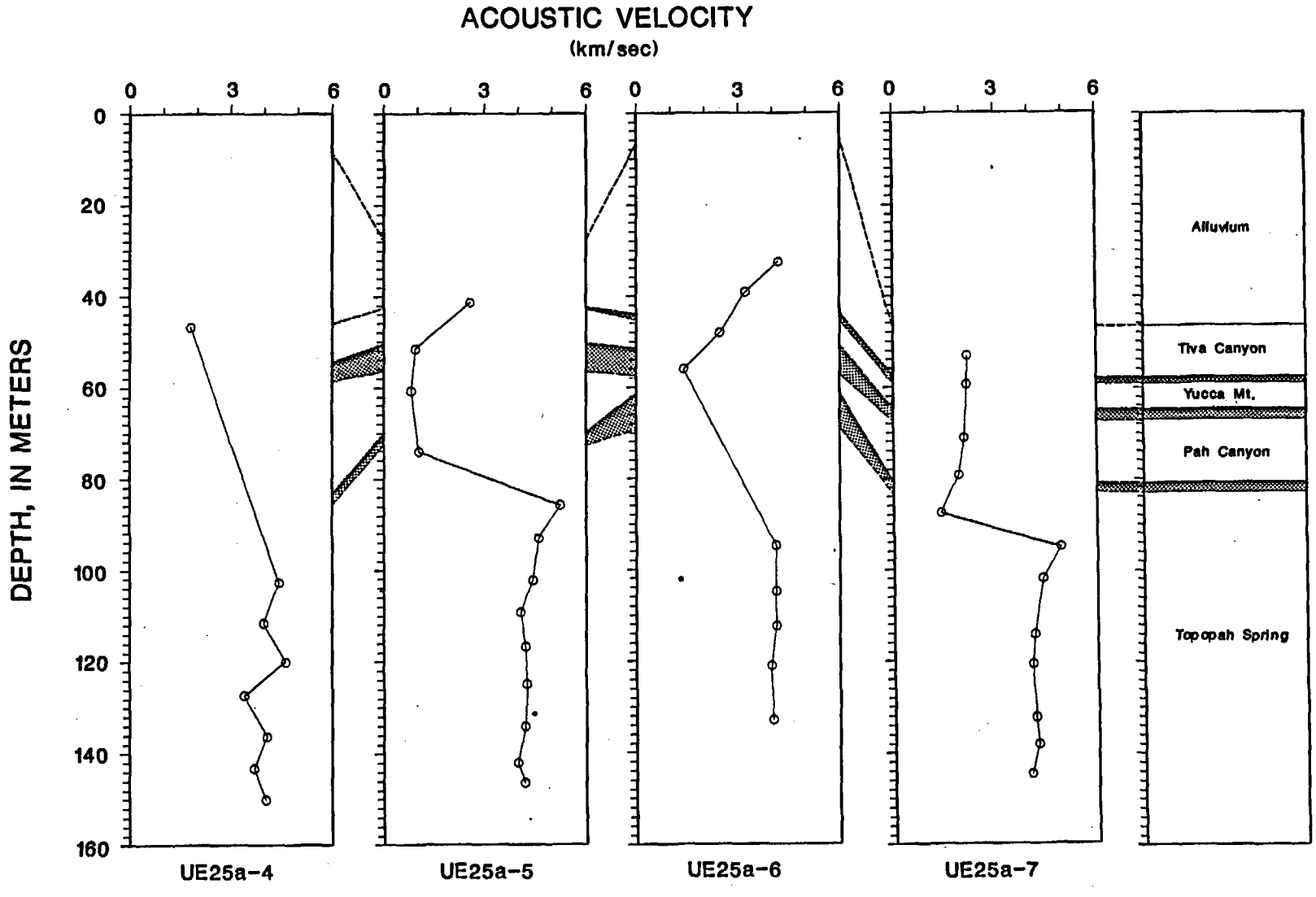

Figure 6. Acoustic velocity plots of sample data obtained on core from the Yucca Mt. UE25a-4, -5, -6, and -7 boreholes.

Topopah Spring Members. The acoustic velocity of the singular Bedded Tuff sample obtained from the UE25a-6 borehole was somewhat higher at 1.4 kilometers/second. Velocities measured on core from the Tiva Canyon Member vary fron 1.8 to 4.2 kilometers/second increasing as a function of welding. The highest values (5.24 and 4.93 kilometers/second) are those associated with the rhyolitic cap rock within the Topopah Spring Member represented in the -5 an -7 boreholes. Samples from below the caprock in the -5, -6, and -7 boreholes show little variation averaging slightly over 4.0 kilometers/second. In borehole -4, sample velocities show greater deviation, possibly as the result of a higher level of vesicularity observed within the rock.

Resisitivity and Magnetic Properties:

The electrical resistance of the borehole samples as received was measured at a frequency of 100 hertz using a Hewlett-Packard digital LCR meter. The procedure was repeated following the resaturation process. Resistance was converted to resistivity using sample length and diameter caliper measurements such that

$$\rho = RA/l$$

where ρ is the sample resistivity in ohm-meters, R is the electrical resistance in ohms, and A and l are the cross-sectional area and length of the sample, respectively.

Magnetic susceptibility (k) was measured directly using a Bison bridge and remanent magnetization (Jr) was obtained with a Schonstedt spinner magnetometer. Both magnetic properties are expressed in Standard International (SI) units.

The measurement results are listed in Table 3. Sample numbers correspond to the depth from which the samples were taken.

Table 3. Values of natural-state and resaturated resistivity made at 100 hertz; magnetic susceptibilty, (k); and remanent magnetization, (Jr), determined for the UE25a-4, -5, -6, and -7 boreholes. Leader (-) indicates sample not suitable for measurement.

Borehole UE25a-4				
Sample Depth in meters (feet)	Natural-State Resistivity	Resaturated Resistivity	k	Jr
	-------ohm-meters----------		(10^{-3} SI)	Amperes/m
46.8 (153.5)	45	48	2.4	0.29
92.9 (304.7)	70	-	-	-
102.8 (337.2)	6600	5500	3.9	1.4
111.6 (366.0)	1400	1000	0.58	0.18
120.0 (393.6)	3600	2200	4.7	0.56
127.3 (417.5)	6200	1500	6.1	0.58
136.3 (447.1)	1800	1300	4.6	0.33
143.3 (470.0)	830	740	5.4	0.64
150.1 (492.3)	620	470	3.9	0.32

Borehole UE25a-5

Sample Depth in meters (feet)	Natural-State Resisitvity	Resaturated Resistivity	k	Jr
	ohm-meters		(10^{-3} SI)	Amperes/m
41.4 (135.8)	19	18	8.1	1.24
51.6 (169.2)	12	-	-	-
60.8 (199.4)	21	-	-	-
69.8 (228.9)	27	-	-	-
74.1 (243.0)	23	-	-	-
85.8 (281.4)	8500	14000	11.0	2.9
93.1 (305.4)	5400	7800	0.99	0.28
102.3 (335.5)	2500	3800	5.9	0.65
109.3 (358.5)	2600	2000	5.2	0.56
116.8 (383.1)	3000	2500	5.4	0.52
124.9 (409.7)	1400	1500	5.8	0.42
134.1 (439.8)	920	840	4.9	0.28
142.0 (465.8)	430	320	3.0	0.29
146.4 (480.2)	670	550	0.67	0.33

Borehole UE25a-6

Sample Depth in meters (feet)	Natural-State Resistivity	Resaturated Resistivity	k	Jr
	ohm-meters		(10^{-3} SI)	Amperes/m
32.7 (107.3)	1400	1600	1.8	0.18
39.3 (128.9)	65	85	19.0	0.76
48.2 (158.1)	60	-	1.81	0.57
56.1 (184.0)	35	-	-	
94.9 (311.3)	1300	1100	5.2	0.56
104.9 (344.1)	1200	1100	3.5	0.32
112.4 (368.7)	770	770	6.2	0.37
121.0 (396.9)	560	550	4.88	0.28
132.9 (435.9)	530	450	0.65	0.21

Borehole UE25a-7

Sample Depth in meters (feet)	Natural-State Resistivity	Resaturated Resistivity	k	Jr
	ohm-meters		(10^{-3} SI)	Amperes/m
53.3 (174.8)	9	9	2.9	0.49
59.6 (195.5)	23	23	4.4	0.73
71.3 (233.9)	23	25	1.3	0.35
79.4 (260.4)	14	-	5.7	0.90
87.6 (287.3)	13	-	-	-
95.2 (312.3)	56000	45000	11.0	1.3
102.1 (334.9)	2500	2200	5.5	0.69
114.4 (375.2)	1200	1100	4.6	0.40
120.8 (396.2)	2100	1300	4.0	0.43
132.4 (434.3)	2400	1400	5.2	0.29
138.3 (453.6)	890	690	5.5	0.51
144.7 (474.6)	540	450	3.4	0.43

The penetrated section at each drill site lies entirely above the static water level. Inasmuch as water fraction within the pore spaces affect the resistivity of the rock, it was considered of interest to measure the resistivity at in situ levels and to compare those values with resistivities of the fully saturated rock. As with the bulk density comparisons, the data are not truly indicative of the resistivity response in the natural environment inasmuch as an unknown amount of desaturation has occurred between the time of extraction from the borehole and time of preservation within its beeswax coating.

The resistivity data in Table 3 has been plotted as a function of sample depth for all four boreholes as shown in figure 7. "Natural-state" sample data are connected by a continuous line and the saturated resistivity values are indicated as single data points. For the non-welded samples from the UE25a-4, -5, and -7 boreholes the natural-state and saturated resistivities are strikingly similar wherever comparisons can be made. According to Spengler and Rosenbaum, 1980, a sufficient quantity of pumice within the rock has been altered to clay thereby creating readily accessible current conduction paths. As a result, pore structure and water saturation levels become less important in controlling the resistivity of the rock.

In the UE25a-6 borehole the Tiva Canyon samples from the 32.7 and 39.3 meter depths have a higher saturated resistivity than that determined for their natural condition. These samples have undergone some degree of welding and are apparently less altered than their nonwelded counterparts. Thus, conduction of electrical current flow is less dependent upon the presence of clay and more dependent upon the amount of water present, the salinity of the water, and its distribution. The observation that the resistivity of these samples is higher in the resaturated state confirms that the natural-state pore waters are more saline than the water used in the resaturation process.

Benson and McKinley, 1985, have made a study of the conductivity of groundwater obtained from 13 boreholes in Yucca Mountain. In terms of resistivity, their results show the water to range from 26 to 35 ohm-meters with most values tending toward the higher end of the specified range. These resistivities are appreciably higher than the 18-22 ohm-meter tap water used in the resaturation process. A rock fully saturated with natural pore waters would then be expected to have a higher resistivity than when in the resaturated state. This observation is true for the samples taken from below the static water level in the USW G-4 borehole but the opposite condition generally exists for the equivalent samples from the USW G-3 borehole (Anderson, 1984). Apparently the pore water resistivity differs between borehole locations and is conceivably less resistant than the recoverable ground waters which flow through the fractures of the rock.

The resistivity of the non-welded samples is 10 to 30 ohm-meters whereas the resistivity of the welded tuff samples from the Topopah Spring Member is typically higher by one to two orders of magnitude. The highest resistivities are associated with the quartz-latite caprock. As seen in figure 7,

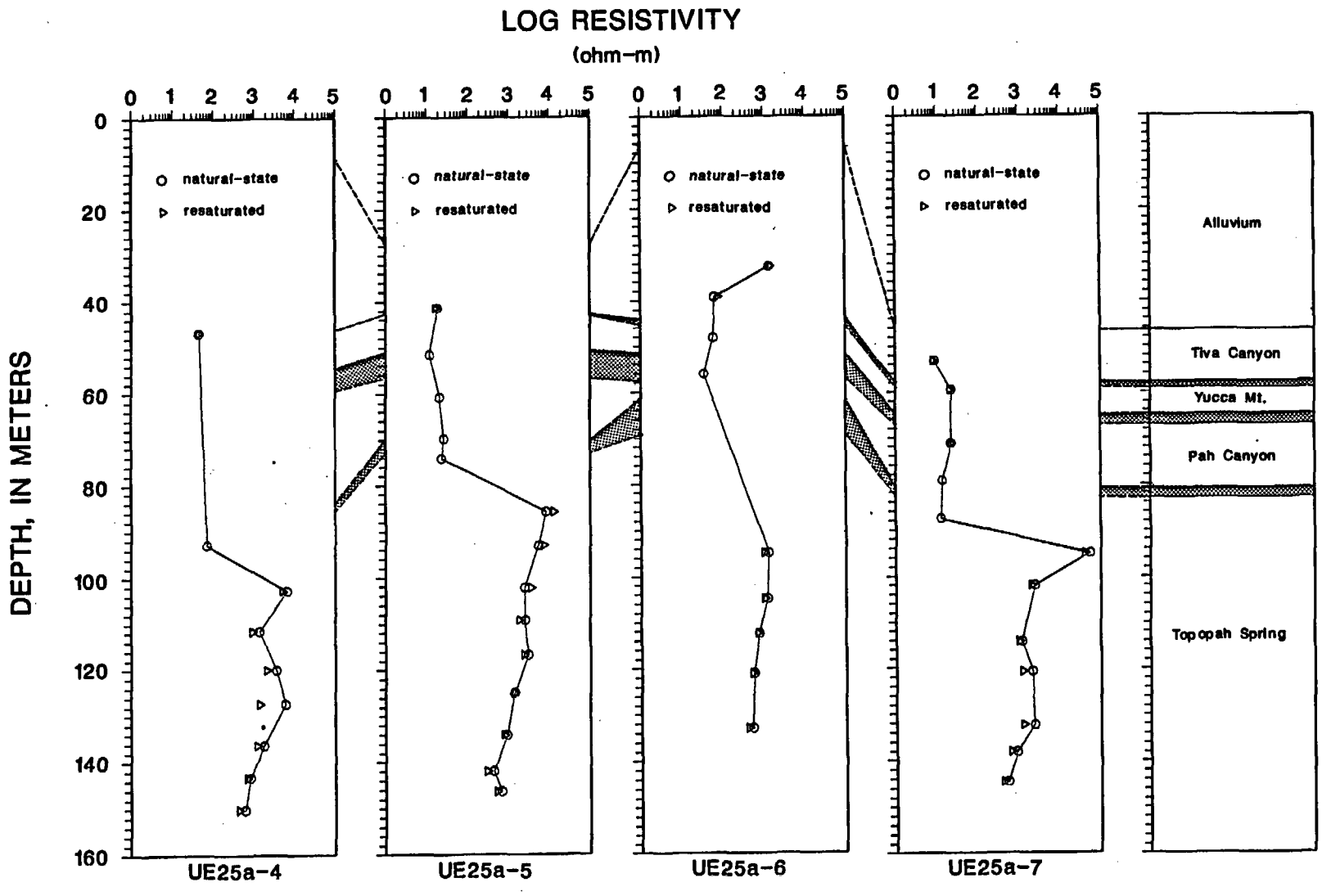

Figure 7. Plots of resistivity data obtained on core samples from the Yucca Mt. UE25a-4, -5, -6, -7 boreholes. Measurements were made on samples containing the original pore waters (circles) and repeated following resaturation (triangles) with local tap water.

particularly for boreholes -4, -5, and -7, resistivities decrease with depth because of a less intense degree of welding within the tuffs (Spengler and Rosenbaum, 1980). Some random variation is evident between the resistivities of the paired samples attributable to differences in saturation levels and pore water resistivity.

Magnetic susceptibility and remanent magnetization values are plotted for all four boreholes in figures 8 and 9, respectively. The magnetic susceptibility of the Tiva Canyon, Yucca Mountain, Pah Canyon, and the nonwelded portion of the Topopah Spring Member is in the range of 0.11 to 11.0 * 10^{-3} SI units; varying as a function of phenocryst abundance and their mafic mineral content. Magnetic susceptibilities of the welded portions of the Topopah Spring Member are somewhat more predictable although exceptions do exist. For example, the quartz-latite samples from the -5 and -7 boreholes (samples 85.8 and 95.2, respectively) have the highest values measured in this tuff member and can readily be distinguished from the underlying rhyolitic tuffs based on their susceptibilities. Borehole -6 lacks a representative quartz-latite sample but in the -4 borehole, sample 102.8 has a susceptibility similar to the remaining welded tuff samples. The lack of continuity in magnetic susceptibiltiy values from one borehole to the next stems from deficiencies in the sampling process rather than from changes in the magnetic properties of the rock at that particular stratigraphic horizon. Continuity in the magnetic susceptibility of the rock has been demonstrated by means of borehole logging (Hagstrom and others, 1980).

The character of the remanent magnetization plots shown in figure 9 is similar to that of magnetic susceptibility. A notable exception is sample 39.3 from the -6 borehole where the susceptibility seems inordinately high relative to its remanence. Corresponding magnetic intensities, however, are not a necessary property of the rock because of a commonly occurring inhomogeneity in the orientation of the permanent magnetization vector within a specified volume of rock.

Of significance is the fact that the intensity of the remanent component is on the order of 2.5 times the intensity of the induced component. The induced component of intensity in amperes/meter is calculated by multiplying the magnetic susceptibility by $(0.52*10^{3})/4\pi$ where 0.52 is the total intensity of the earth's magnetic field in oersteds at the Yucca Mountain location. In addition, the remanent vector directions are inverse to the present day's earth's field within the Tiva Canyon, Pah Canyon , and the Yucca Mountain Members causing a very complicated near-surface magnetic field distribution at the Drill Hole Wash site.

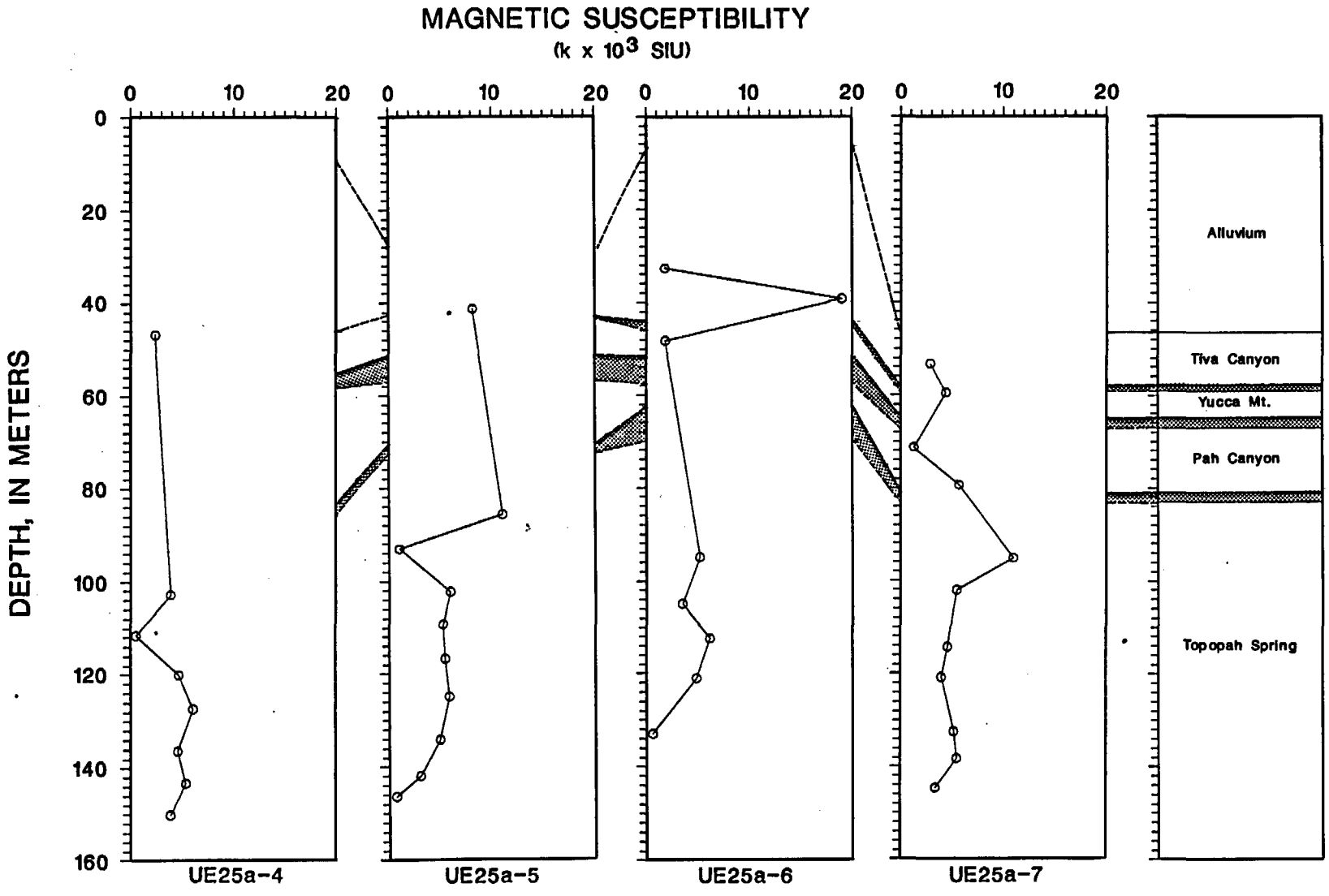

Figure 8. Plots of magnetic susceptibility values obtained on core samples taken from the Yucca Mt. UE25a-4, -5, -6, and -7 boreholes.

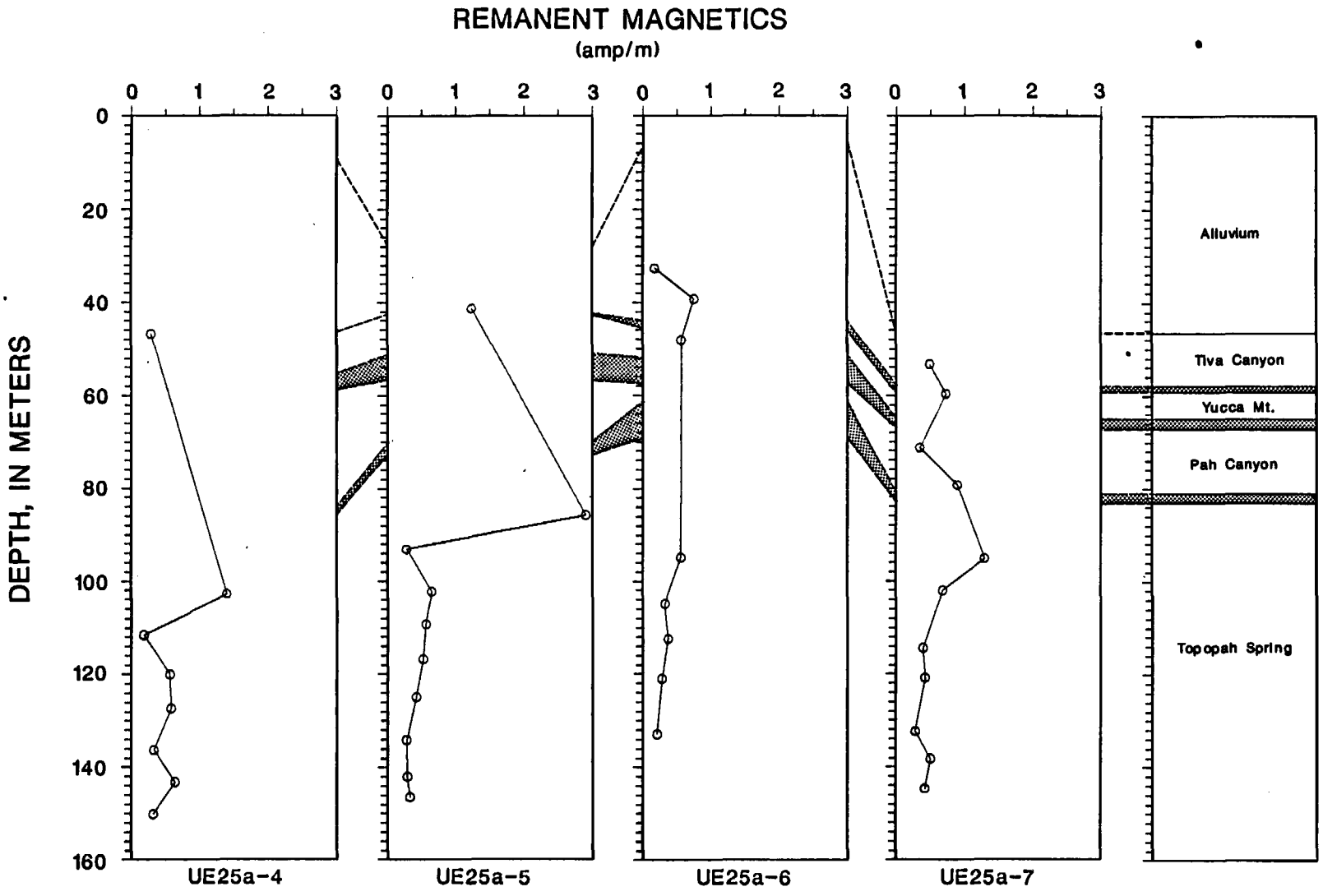

Figure 9. Plots of remanent magnetization values obtained on core samples taken from the Yucca Mt. UE25a-4, -5, -6, and -7 boreholes.

Summary

Core samples from four members of the Paintbrush Tuff were collected from a series of shallow boreholes located in the Drillhole Wash area of Yucca Mountain. Although many samples were poorly consolidated, particularly those from the Yucca Mountain and Pah Canyon Members, in every case, their structural competence was sufficient to permit bulk density and resistivity measurements to be made on core containing the original pore waters. When sample resaturation was attempted, many disintegrated, limiting the number of rock properties evaluated on many samples to the two just mentioned. However, based on the fragile nature of these highly friable rock sections, readily identified by their low bulk density and resistivity, the textural character of the rock, including the bedded tuff intervals, is one of a highly open pore structure offering little in the way of an impediment to ground water flow.

Repeat measurements of bulk density on the more competent samples following resaturation indicate that, in virtually every instance, the resaturated density is greater than the "natural-state" density. This is an expected result in that the rock exists above the static water level and is presumed to be undersaturated. Also, it is likely that some water loss occurred during the period between withdrawal from the borehole and the final wrapping process.

The effect of the undersaturated condition is, however, not readily apparent from the results of the combined resistivity measurements. For those samples having porosities in excess of 25 percent, the resistivities are essentially the same in both saturation modes; an indication that current flow through the sample is more dependent on surface conduction than on pore water resistivity. Conversely, the resaturated resistivity of the samples representing the Topopah Spring Member are typically less than that of the "natural-state" resistivity demonstrating that conduction is primarily by means of current flow within the water occupying the pore spaces of the rock. The Topopah Spring samples on which dual resistivity measurements were made have all been welded to some degree resulting in pore size diameters not amenable to water migration through the rock. Consequently, the tuff has been subjected to clay alteration and possibly zeolite formation to a much lesser extent. For virtually all Topopah Spring samples the resistivity differences between saturation modes are not significant suggesting a continuity in pore water distribution of the rock in the in place environment. Where wide disparities in resistivity values exist, it is assumed that the core suffered some level of dehydration following its removal from the borehole.

Samples from the UE25a-5 borehole taken from the 85.8, 93.1, and 102.3 meter depths are atypical of the resistivity responses observed in the Topopah Spring core. In all three samples the resistivity increased following resaturation which possibly was caused by failure to achieve complete saturation. The 85.8 and 93.1 samples have measured porosities of 2.9 and 4.2 percent, respectively, therefore it is conceivable that minute changes in the volume and distribution of the pore water could result in significant changes in resistivity from that measured containing the original pore waters. The reason for the higher resistivity of the 102.3 meter depth sample in its resaturated state is not readily apparent inasmuch as the sample porosity is 11.4 percent and considered to be less susceptible to resistivity changes as a function of very small variations in the volume of pore water contained within

the rock. High pore water salinity in the in place environment may occur within the interval affecting the 85 to 102.3 meter samples but there is no evidence that an isolated occurrence of this nature can exist.

A summary of the average rock property values determined for rock types within the respective stratigraphic units is as follows (NBD, "natural-state" bulk density; SBD, saturated bulk density; DBD, dry bulk density; GDA and GDH, grain density by water and helium invasion methods, respectively; ϕ, porosity; Vp, compressional sonic velocity; kd, water permeability; ρ_n, "natural-state" resistivity; ρ_r, resaturated resistivity; K, magnetic susceptibility; and Jr, remanent magnetization):

Yucca Mountain: (non-welded)

Rock Property		UE25a-4	UE25a-6	UE25a-7
NBD	(Mg/m^3)	1.56	1.57	1.53
SBD	"	1.74	-	1.65
DBD	"	1.33	-	1.09
GDA	"	2.26	-	2.46
GDH	"	2.31	2.34	2.34
ϕ	(percent)	41.2	-	55.5
Vp	(km/sec)	1.80	2.46	2.18
kd	(millidarcies)	2480	4170	202
ρ_n	(ohm-meters)	45	60	23
ρ_r	"	48	-	23
K	(SIU)	2.4	1.81	4.4
Jr	(Amp/m)	0.29	0.57	0.73

Tiva Canyon: (n, non-welded: p, partially welded; pm, partially-to-moderately welded)

Rock Property		UE25a-4 (n)	UE25a-6 (p)	UE25a-6 (pm)	UE25a-7 (n)
NBD	(Mg/m^3)	1.87	1.97	2.32	1.90
SBD	"	1.88	1.99	2.33	1.92
DBD	"	1.46	1.70	2.23	1.49
GDA	"	2.53	2.39	2.49	2.60
GDH	"	2.44	2.44	2.46	2.47
ϕ	(percent)	42.2	28.9	10.5	42.8
Vp	(km/sec)	2.59	3.22	4.21	2.19
kd	(millidarcies)	3.10	.077	.051	1430
ρ_n	(ohm-meters)	19	65	1400	9
ρ_r	"	18	85	1600	9
K	(SIU)	8.1	19.0	1.8	2.9
Jr	(Amp/m)	1.24	0.76	0.18	0.49

Pah Canyon: (non-welded)

Rock Property	UE25a-5	UE25a-7
NBD (Mg/m^3)	1.61	1.52
SBD "	-	1.60
DBD "	-	1.17
GDH "	2.37	2.38
ϕ (percent)	-	43.1
Vp (km/sec)	0.81	2.02
kd (millidarcies)	-	197
ρ_n (ohm-meters)	24	23
ρ_r "	-	25
K (SIU)	-	3.5
Jr (Amp/m)	-	0.63

Bedded Ash-Flow Tuff:

Rock Property	UE25a-5	UE25a-6
NBD (Mg/m^3)	1.73	1.56
GDH "	2.34	2.39
Vp (km/sec)	0.93	1.40
ρ_n (ohm-m)	12	35

Topopah Spring: (non-welded)

Rock Property	UE25a-4	UE25a-5	UE25a-7
NBD (Mg/m^3)	1.59	1.69	1.54
GDH "	2.39	2.41	-
Vp (km/sec)	-	1.03	1.41
ρ_n (ohm-m)	70	23	13

Topopah Spring: (densely welded)

Rock Property	UE25a-4	UE25a-5	UE25a-6	UE25a-7
NBD (Mg/m^3)	2.28	2.30	2.27	2.30
SBD "	2.36	2.35	2.33	2.37
DBD "	2.23	2.24	2.18	2.25
GDA "	2.55	2.53	2.55	2.56
GDH "	2.55	2.53	2.55	2.54
ϕ (percent)	12.6	11.6	14.5	12.2
Vp (km/sec)	4.02	4.35	4.07	4.29
kd (millidarcies)	6.04	0.23	0.73	1.05
ρ_n (ohm-m)	2410	2820	870	9380
ρ_r "	1200	3700	790	7450
K (SIU)	4.21	4.76	4.09	5.60
Jr (Amp/m)	0.44	0.69	0.35	0.58

Rock properties such as resistivity, bulk density, porosity, compressional sonic velocity, and permeability clearly vary as a function of the degree of welding to which the rock has been subjected. Higher values of resistivity, sonic velocity, and density are typically associated with densely welded tuff; the inverse being true for the non-welded sections. Porosities are relatively high in the poorly consolidated subunits of the Paintbrush Tuff and moderate within the welded portions. Porosity, however, provides no clue as to the water permeability of the rock inasmuch as the latter is apparently controlled by the size of the pore spaces within the groundmass of the tuffs. Magnetic measurements indicate the ratio of the remanent component to the induced to be about 2.5.

Part 2. Rock property measurements on core samples obtained from the UE25p#1 borehole.

Introduction

Borehole UE25p#1 was emplaced at a site approximately 3 km east of Yucca Mt. as shown in figure 1. The hole was drilled primarily for the purpose of investigating the character of a section of the Paleozoic rocks underlying the tuffaceous beds of the Yucca Mt. structural block (Carr and Others, 1986). Sixteen core samples were obtained from the 1052 - 1799 meter depth interval. The two uppermost samples represent Miocene tuffs of the Yucca Mountain series; 13 samples were taken from the Lone Mountain Dolomite formation; and a single sample was obtained from the Roberts Mt. Formation which is also a dolomite. According to the Carr report, the dolomites are Late Silurian in age. Laboratory and analytical procedures used in determining the physical properties of the rock are exactly those described in Part 1 for the UE25a-4, -5, -6, -7 boreholes. Sample numbers correspond to the depth interval from which they were taken.

Laboratory Results

Density, Porosity, Permeability, and Compressional Sonic Velocity:

Bulk and grain density values determined for the individual core samples are listed in Table 4. The stratigraphic unit from which each sample was taken is also indicated.

Table 4. Calculated values of bulk and grain density obtained for the UE25p#1 borehole samples. NBD, SBD, DBD, and GDA, represent natural-state bulk density, saturated bulk density, dry bulk density, and grain density, respectively, using bulk and grain volume determined by the bouyancy method; GDH is grain density using grain volume determined by helium pycnometry on bulk samples. The stratigraphic units from which the individual samples have been taken are also identified.

Sample depth in meters (feet)	NBD	SBD	DBD	GDA	GDH	Stratigraphic Unit
			Mg/m^3			
1052.7 (3452.9)	2.28	2.28	2.10	2.56	2.54	Lithic Ridge Tuff
1194.2 (3917.0)	2.41	2.44	2.28	2.71	2.63	Calcified Tuff
1282.8 (4207.6)	2.78	2.79	2.75	2.87	2.86	Lone Mt. Dolomite
1303.2 (4274.5)	2.77	2.77	2.72	2.86	2.85	"
1309.7 (4295.8)	2.76	2.76	2.71	2.86	2.85	"
1331.9 (4368.6)	2.81	2.81	2.78	2.86	2.86	"
1347.4 (4419.5)	2.83	2.83	2.82	2.86	2.85	"
1360.2 (4461.5)	2.67	2.67	2.57	2.86	2.85	"
1373.3 (4504.4)	2.75	2.75	2.69	2.85	2.85	"
1388.8 (4555.3)	2.75	2.75	2.70	2.86	2.86	"
1406.6 (4613.6)	2.68	2.68	2.59	2.86	2.86	"
1421.8 (4663.5)	2.83	2.83	2.82	2.86	2.85	"
1433.8 (4702.9)	2.82	2.82	2.81	2.85	2.85	"
1455.3 (4773.4)	2.83	2.83	2.82	2.85	2.84	"
1483.0 (4864.2)	2.80	2.80	2.77	2.86	2.86	"
1799.0 (5900.7)	2.84	2.84	2.83	2.84	2.83	Roberts Mt. Fm.

Bulk densities for the "natural-state" and resaturated samples are plotted in figure 10 along with the lithology as derived from Carr and others, 1986. Except for the Calcified Tuff sample, which apparently experienced some water loss upon withdrawal from the borehole, the data sets are equivalent indicating that the core was fully saturated at the time of preservation. The textural properties of the Lithic Ridge tuff sample are akin to those values obtained on samples from the same unit within the Yucca Mt. USW G-3 borehole (Anderson, 1984). The Calcified Tuff section has not been encountered elsewhere in Yucca Mt. drillholes.

Much of the Lone Mt. Dolomite has been brecciated and recemented with secondary dolomite. In those intervals where the cementation is incomplete the bulk densities are lowest in value. The high density values can be correlated with crystalline dolomite. The Roberts Mt. dolomite sample falls within the latter classification.

As seen in figure 11 the grain density of the Lone Mt. Dolomite determined by both helium and water invasion techniques is essentially the same despite the much smaller volume of rock used with the helium pycnometer method. Grain densities are reasonably uniform for the dolomite samples averaging about 2.85 Mg/m^3. The grain density of the Roberts Mt. dolomite is slightly lower at 2.83 Mg/m^3.

Grain densities of the tuff samples are higher as measured by water invasion than those values obtained by helium pycnometry. This observation is unusual in that the latter method typically results in a smaller rock volume and a resulting higher grain density as compared to those determined by the water invasion method. Apparently the phenocryst and lithic fragment distribution within the tuffs is nonuniform resulting in perceptible differences in grain density as a function of sample size. However, the grain density value obtained by each method is considered to be accurate for the sample volume used in the measurement.

Porosity, water permeability, and compressional sonic velocity values determined for the UE25p#1 borehole are listed in Table 5.

Figure 12 is a plot of the sample porosities listed in Table 5. Porosities of the partially welded tuffs are substantially higher than those of the dolomite samples. Some reduction in the porosity of the Calcified Tuff sample has apparently resulted from the introduction of calcite into the vugs and pore spaces of the tuff.

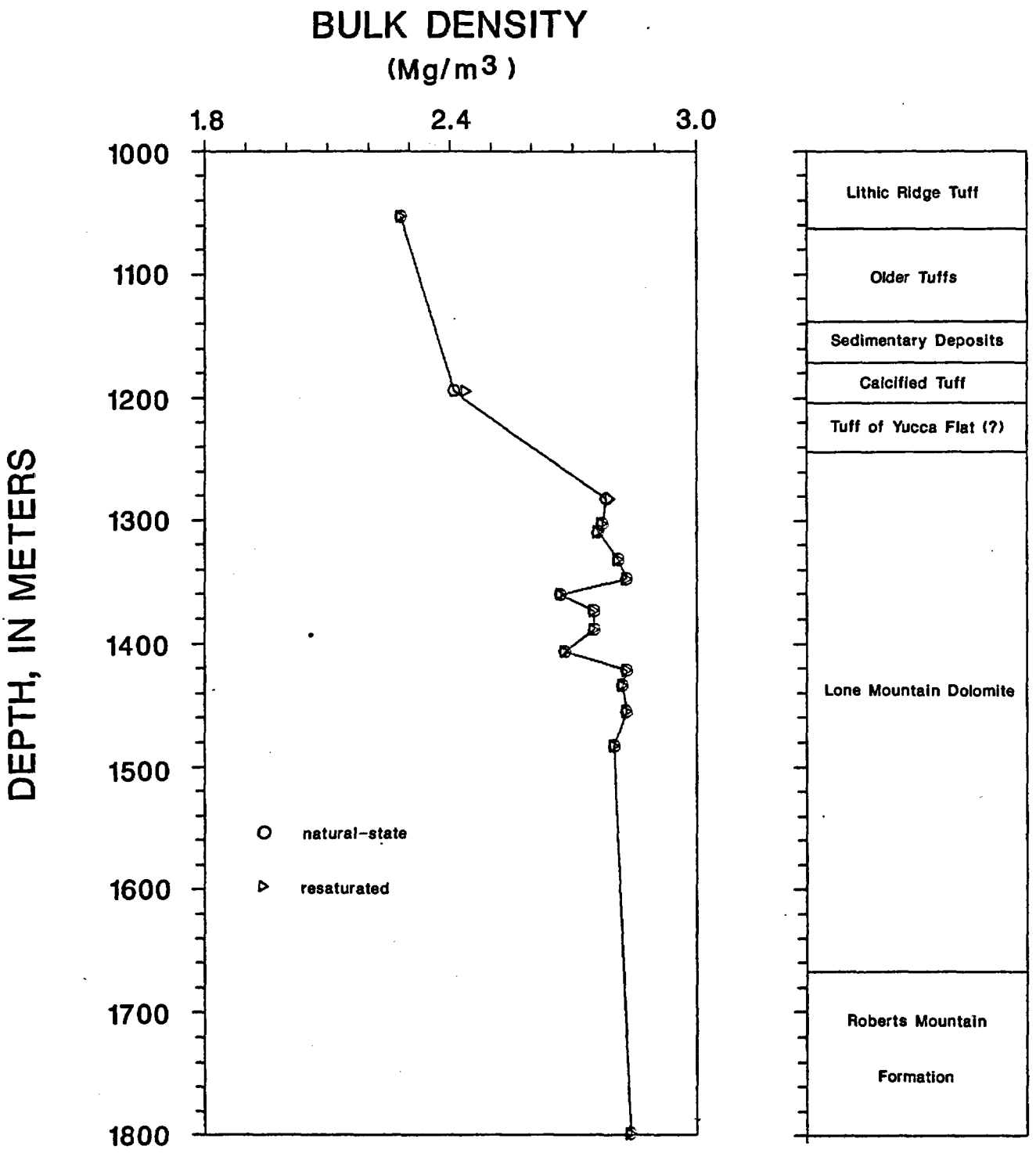

Figure 10. Plot of bulk density values determined for core samples from the UE25p#1 borehole. Circles designate in place levels of pore water within the rock and the triangles indicate values obtained following resaturation with local tap water. The stratigraphic section as presented by Carr and Others, 1986, is shown on the right-hand side of the figure.

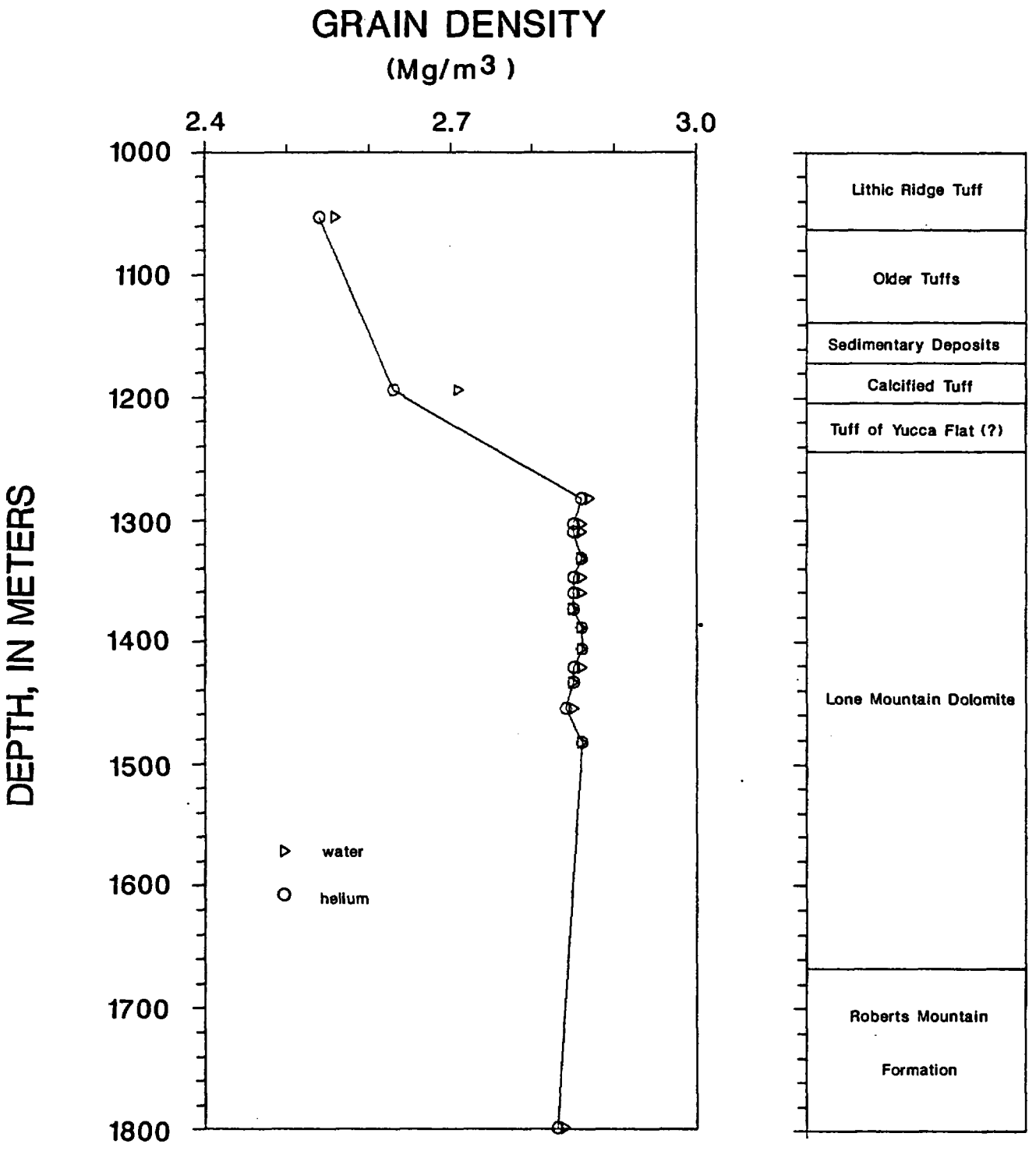

Figure 11. Plot of grain density values for the UE25p#1 borehole core samples using rock volumes determined by both helium and water displacement methods.

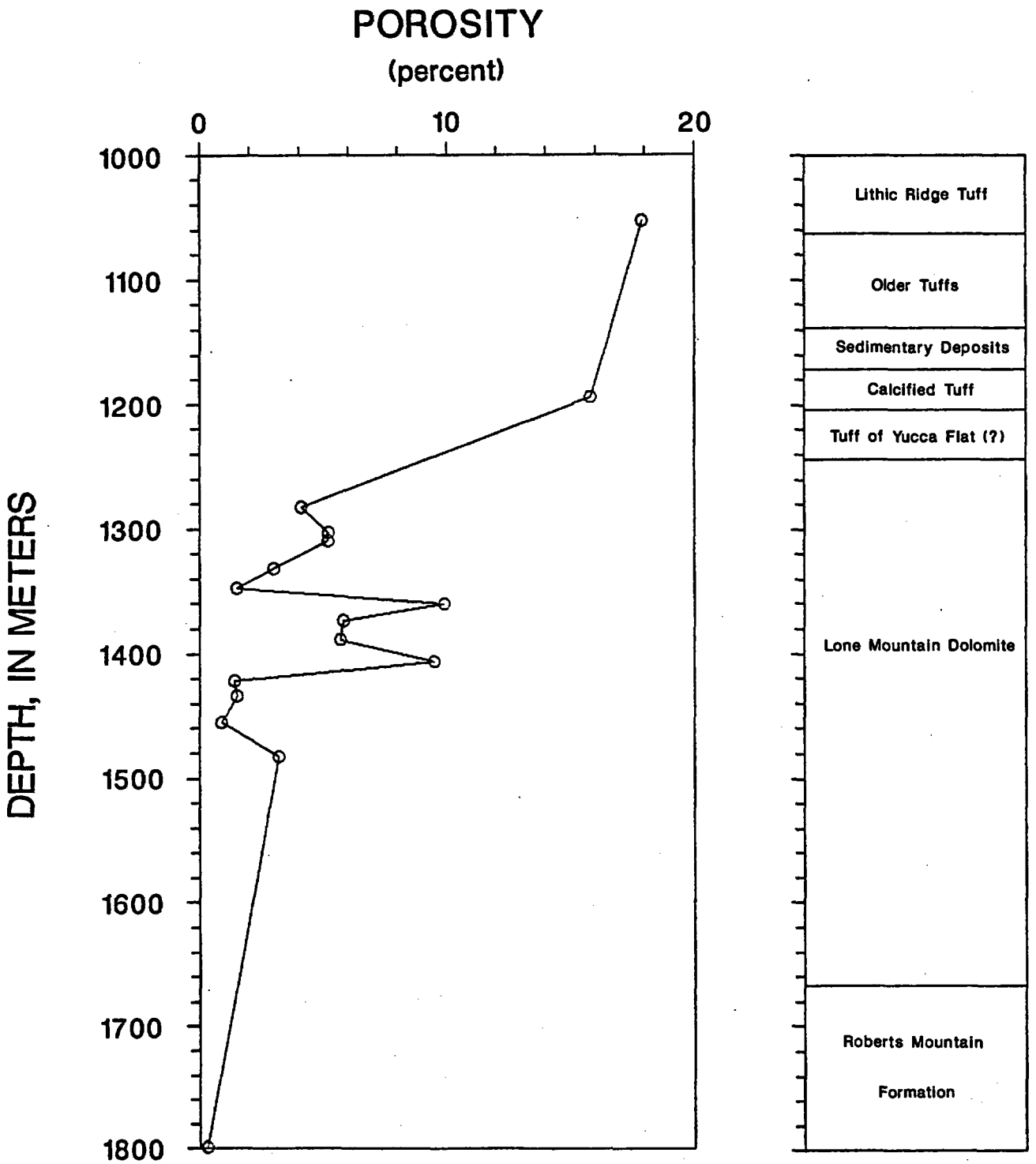

Figure 12. Plot of porosity values determined for the UE25p#1 borehole samples.

Table 5. Calculated values of water accessible porosity,; permeability, kd, measured in the vertical (v) and horizontal (h) flow directions; and compressional sonic velocity, Vp; obtained for the UE25p#1 borehole samples. Leader (-) indicates sample was not suitable for measurement.

Sample Depth in meters (feet)	Porosity in percent	kd(v) millidarcies	kd(h)	Compressional Sonic Velocity in km/sec.
1052.7 (3452.9)	17.9	.087	.11	3.54
1194.2 (3917.0)	15.8	32.8	-	2.44
1282.8 (4207.6)	4.1	2.8	-	4.46
1303.2 (4274.5)	5.2	.98	.575	4.60
1309.7 (4295.8)	5.2	.16	.16	4.74
1331.9 (4368.6)	3.0	-	.76	4.91
1347.4 (4419.5)	1.5	.0025	.305	5.18
1360.2 (4461.5)	9.9	164.0	29.0	4.15
1373.3 (4504.4)	5.8	-	-	4.53
1388.8 (4555.3)	5.7	1.650	5.24	4.42
1406.6 (4613.7)	9.5	3.78	8.65	3.96
1421.8 (4663.5)	1.4	.0089	.08	5.06
1433.8 (4702.9)	1.5	-	.015	4.99
1455.3 (4773.4)	0.9	.037	.00063	5.19
1483.0 (4864.2)	3.2	3.87	2.22	4.68
1799.0 (5900.7)	0.3	.034	.0021	5.28

Within the Lone Mountain Dolomite porosities are highest in the brecciated samples indicating that the pore fraction of the whole rock occurs primarily within the secondary dolomite fill material. The non-brecciated samples have porosities of less than two percent. Fractures within the Lone Mountain and Roberts Mountain dolomites are filled with crystallized calcite thus contributing little to the total porosity of the rock.

Permeabilities were determined for vertically and horizontally oriented core drilled from the original borehole sample (figure 13). Because of the orientation of open fractures not all samples were suitable for the measurement.

The permeabilities of the relatively high porosity Lithic Ridge Tuff samples are quite low attesting to their very fine matrix pore structure. The Calcified Tuff, as measured in the vertical flow direction, has a high permeability attributed to microfractures rather than pore structure. Permeabilities of the Lone Mountain Dolomite samples vary as a function of the degree to which the rock has been brecciated indicating that water transport is primarily through the fracture-filling secondary dolomite. Fractures in the non-brecciated crystalline dolomite contribute to the permeability of the rock to a much lesser extent. As an example, little difference in permeability values are evident when comparing the results obtained on the horizontally aligned core from the 1347.4 and 1421.8 meter depths. The 1421.8 sample is essentially fracture-free whereas the 1347.4 sample contains an abundance of microfractures. Variations in permeability between paired samples from a given depth are believed to be caused by fracture orientation.

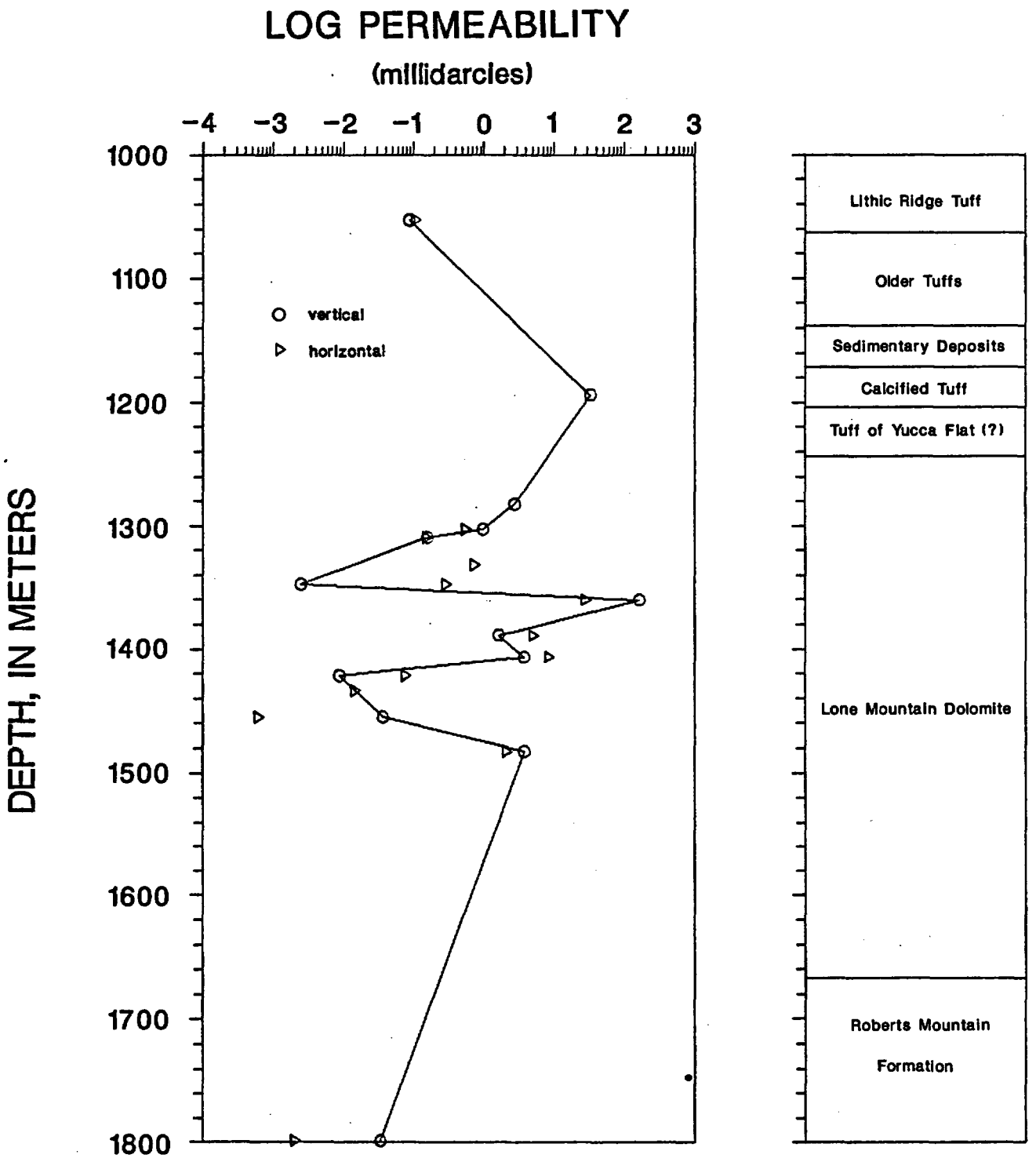

Figure 13. Plot of permeability values determined for vertical and horizontal flow directions on samples taken from the UE25p#1 borehole.

The sonic velocity plot (figure 14) is virtually a mirror image of the porosity plot. The obvious exception is the Lithic Ridge Tuff sample which has a high porosity and a correspondingly high velocity. To test the porosity/velocity relationship, the least squares method was applied to the data using porosity as the independent variable (figure 15). The dolomite samples conform reasonably well to the formulated regression line but both tuff samples, at the high end of the porosity scale, deviate widely from the trend set by the line. Possibly the continuity of the fine-grained groundmass of the partially welded Lithic Ridge sample is sufficient to provide an unimpeded travel path for the acoustic energy with little interference from the larger pore structures and small percentage of contained lithic fragments. The result is a higher than predicted sonic velocity. In contrast, the Calcified Tuff sample deviates from the regression line in a negative sense; the velocity much lower than predicted from the regression line for the specified porosity. The Calcified tuff is also partially welded and, according to Carr and Others, 1986, most of the original phenocryst minerals have been replaced by calcite so as to occupy more than 50 percent of the rock volume. Although the texture of the Calcified Tuff groundmass is similar to that of the Lithic Ridge Tuff, the presence of calcite nodules dispersed along the sonic energy travel path may be sufficient to cause an appreciable level of energy attenuation at the calcite/tuff interfaces. These samples may be atypical in that a like procedure applied to a substantially larger number of tuff samples from the USW G-4 and USW GU-3/G-3 boreholes clearly established a velocity dependence on the porosity of the samples (Anderson, 1984).

Resistivity and Magnetic Properties:

Resistivity, magnetic susceptibility, and remanent magnetization were determined as described in Part 1. The results are listed in Table 6.

Table 6. Values of natural-state and resaturated resistivity made at 100 hz.; magnetic susceptibility, (k); and remanent magnetization, (Jr), determined for the UE25p#1 borehole samples. Leader (-) indicates sample not suitable for measurement.

Sample Depth in meters (feet)	Natural-state Resistivity	Resaturated Resistivity	$k*10^6$	$Jr*10^6$
	ohm-meters		(SIU)	(Amp/m)
1052.7 (3452.9)	185	185	160	3390
1194.2 (3917.0)	28	26	115	413
1282.8 (4207.6)	550	900	21.6	351
1303.2 (4274.5)	590	970	17.3	349
1309.7 (4295.8)	970	1300	25.0	446
1331.9 (4368.6)	850	1400	21.4	188
1347.4 (4419.5)	6100	9100	23.0	186
1360.2 (4461.5)	500	750	14.0	8.7
1373.3 (4504.4)	300	580	-	-
1388.8 (4555.3)	350	1100	19.0	77.7
1406.6 (4613.6)	660	900	15.7	45.1
1421.8 (4663.5)	3000	4200	27.6	336
1433.8 (4702.9)	1720	2200	33.7	870
1455.3 (4773.5)	2700	3600	53.5	1280
1483.0 (4864.2)	700	2300	16.0	49.6
1799.0 (5900.7)	41000	13000	27.9	529

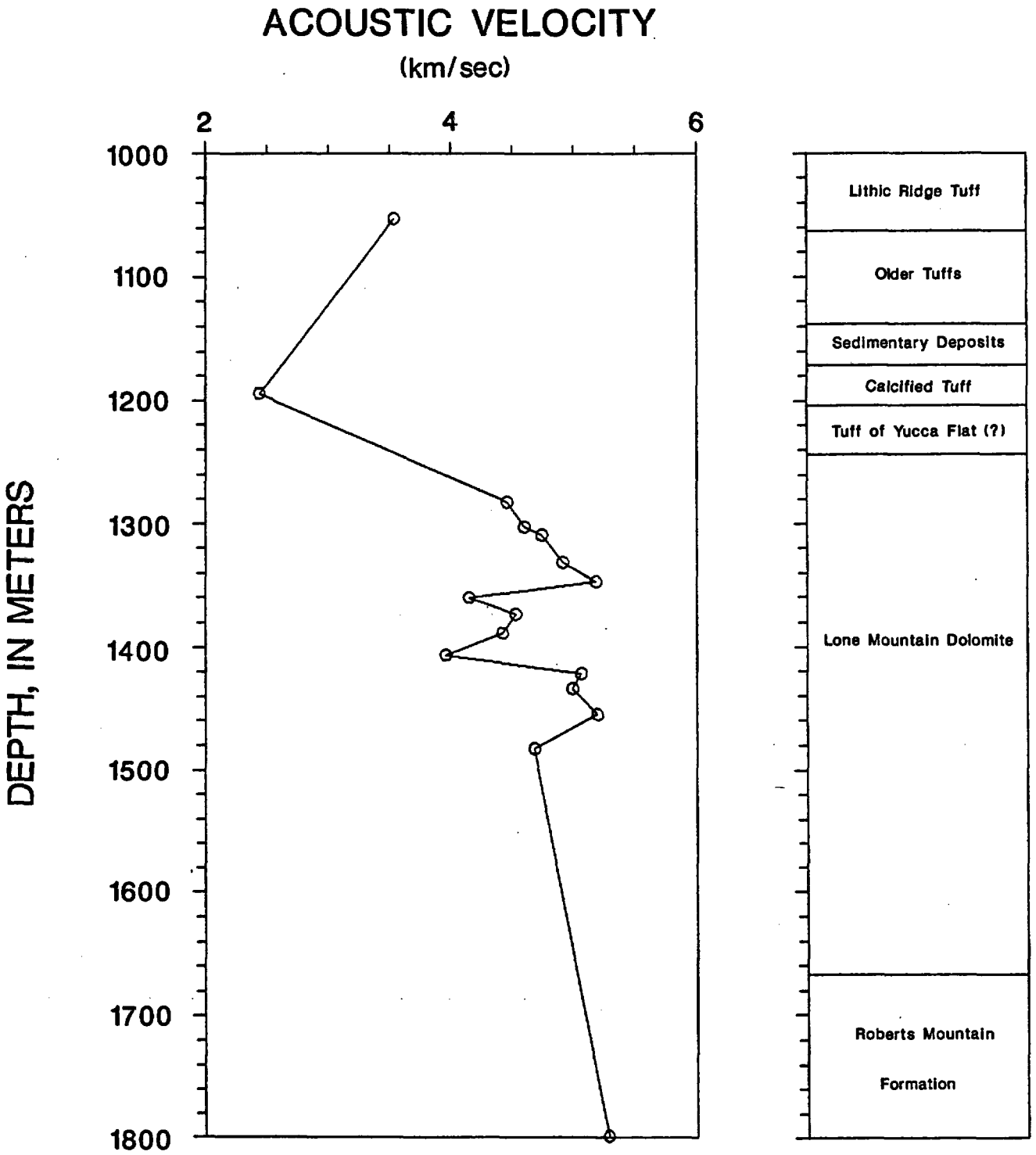

Figure 14. Plot of sonic velocity data obtained on core samples from the UE25p#1 borehole.

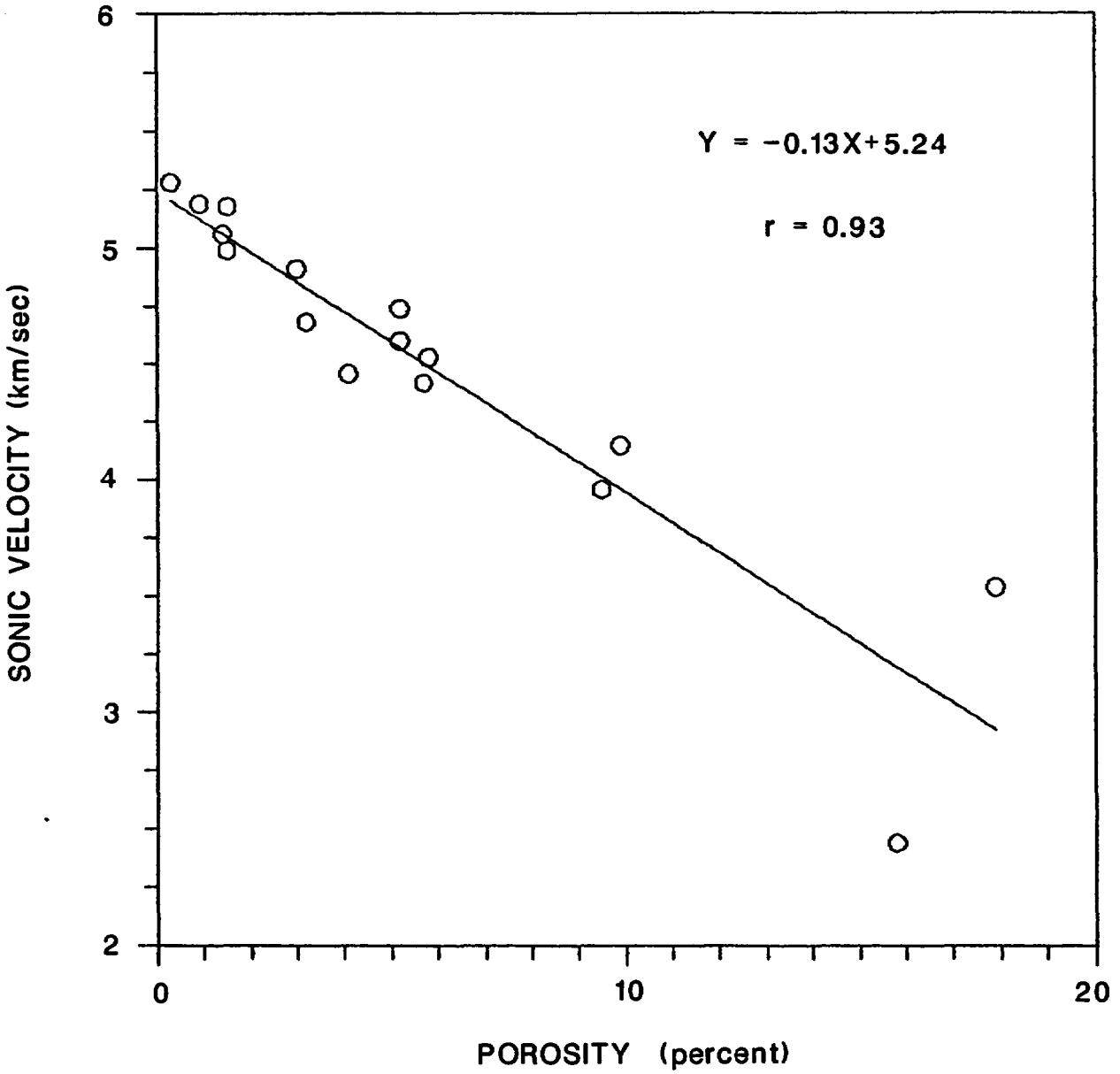

Figure 15. Correlation between the sonic velocity and porosity data determined for the UE25p#1 borehole samples based on a least squares fit. The equation for the line of regression and the correlation coefficient, r, is indicated on the plot.

The resistivity data listed in Table 6 have been plotted in figure 16; the "natural-state" resistivities are connected by a continuous line and the resistivities of the resaturated samples shown as single data points. Resistivity values are the same for the tuffs in both saturation states. Resistivities of the Lone Mountain Dolomite samples containing natural pore waters are always lower than those measured following the resaturation process. The differences are caused by the formation of the dolomites in a marine environment leading to the capture of high salinity waters within the pore spaces of the rock. Apparently the Roberts Mountain dolomite sample underwent some level of dehydration between the time of extraction from the borehole and the time of wrapping inasmuch as the "natural-state" resisitivity is substantially higher than the resistivity in the resaturated state.

Resistivity varies largely as a function of porosity, pore water salinity, level of water saturation within the pore spaces, and the presence of clays and zeolites within the rock. In high salinity rocks, the surface conduction caused by clays and zeolites is substantially subdued and not a strong influencing factor in controlling the resistivity of the rock. As with sonic velocity, the controlling effect of porosity can be correlated with the variations indicated on the resistivity plot.

A least squares line fitted to the resistivity/porosity data using resistivity values obtained on samples saturated with in place pore waters is shown in figure 17. The relationship between the two variables is non-linear and best described by the logarithmic equation specified on the figure. The data fit is reasonably good as indicated by the regression coefficient. As in the sonic velocity/porosity plot, the higher porosity tuff samples deviate from the line of regression in the same manner. Possibly the resistivity of the Lithic Ridge Tuff sample is higher than predicted by the regression line because of some degree of discontinuity in the pore water distribution within the voids of the rock. In contrast, the resistivity of the Calcified Tuff is anomalously low. From the description of the core offered by Carr and Others, 1986, the low resistivity of the Calcified Tuff may be caused by alignments of flattened, argillized pumice within the sample.

Magnetic susceptibility and remanent magnetization plots are shown in figures 18 and 19, respectively. The susceptibility of the dolomite samples averages 24 x 10^6 SI units, a factor of at least 4 less than that determined for the overlying tuffs. An increase in the magnetic mineral content of the rock occurs within the interval defined by the samples taken from the 4702.9 and 4773.5 meter depths.

The plot of remanent magnetization is very similar to that of magnetic susceptibility. Remanent intensity values of the dolomite samples vary from 0.7 to 1280 x 10^6 Amperes/meter; the highest value a factor of three less than the remanence of the Lithic Ridge Tuff.

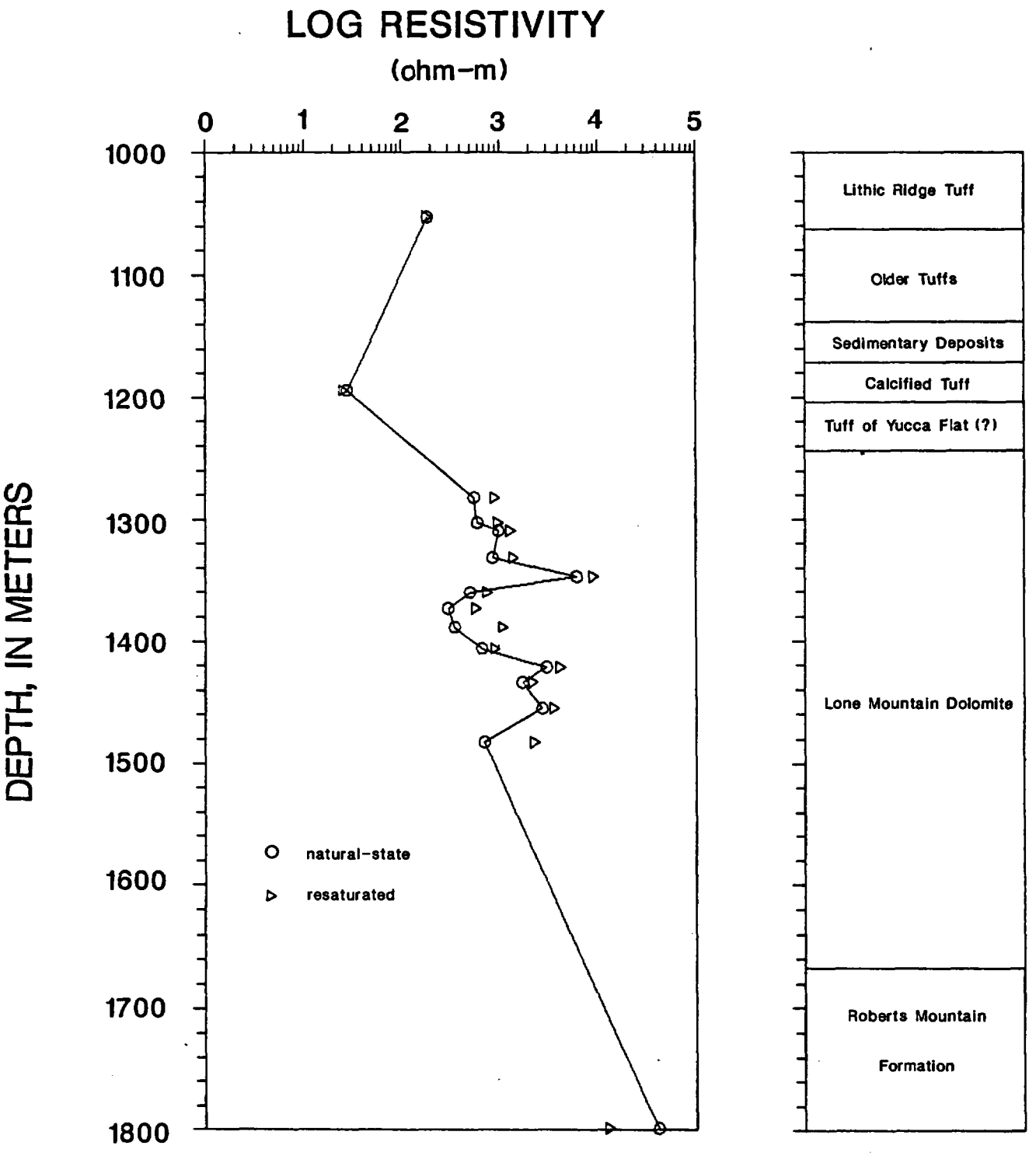

Figure 16. Resistivity plots for UE25p#1 borehole samples measured when containing in place levels of pore water and repeated following resaturation with local tap water.

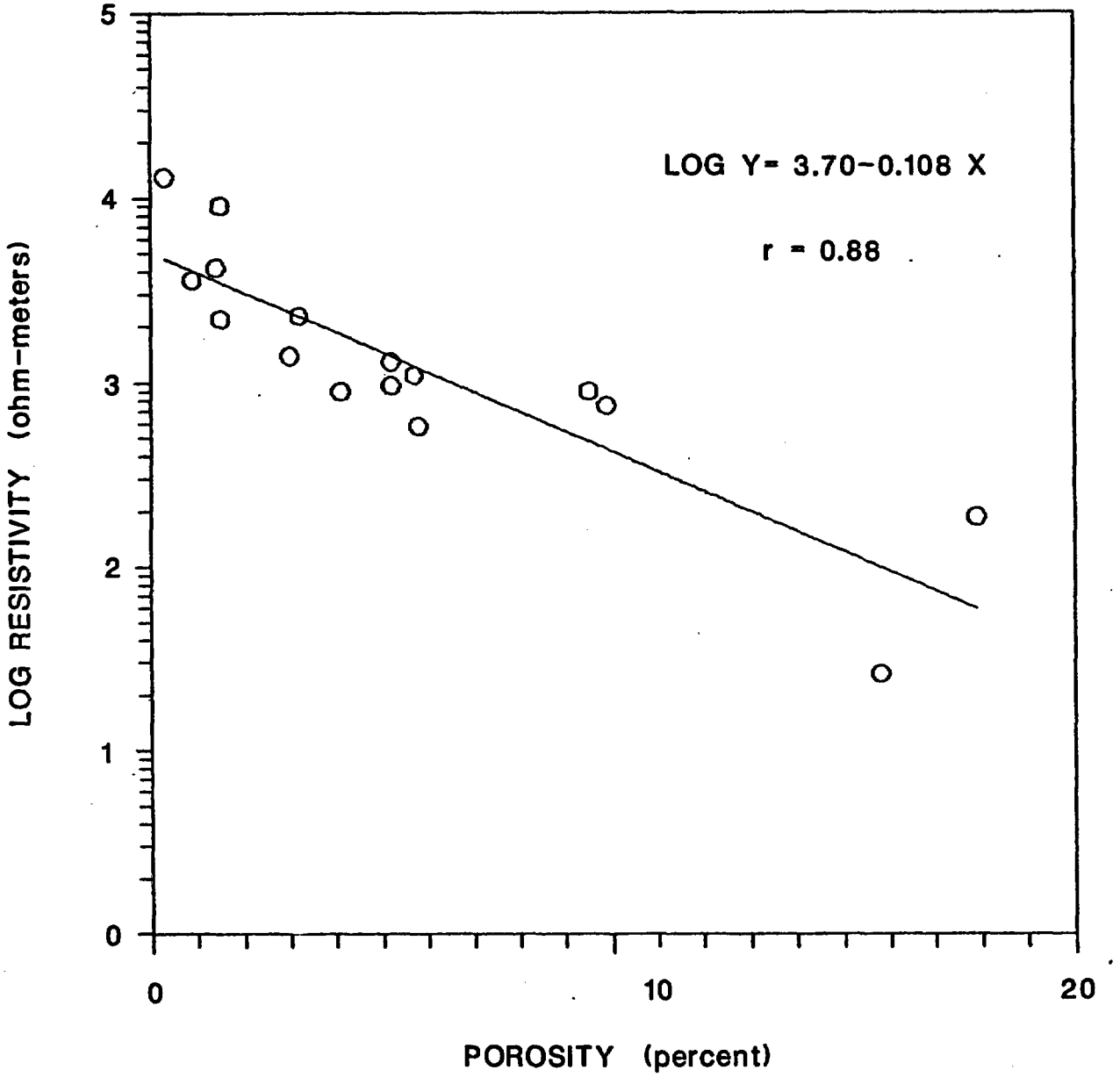

Figure 17. Correlation between resistivity and porosity data determined for the UE25p#1 borehole samples based on a least squares fit. The equation for the line of regression and the correlation coefficient, r, is indicated on the plot.

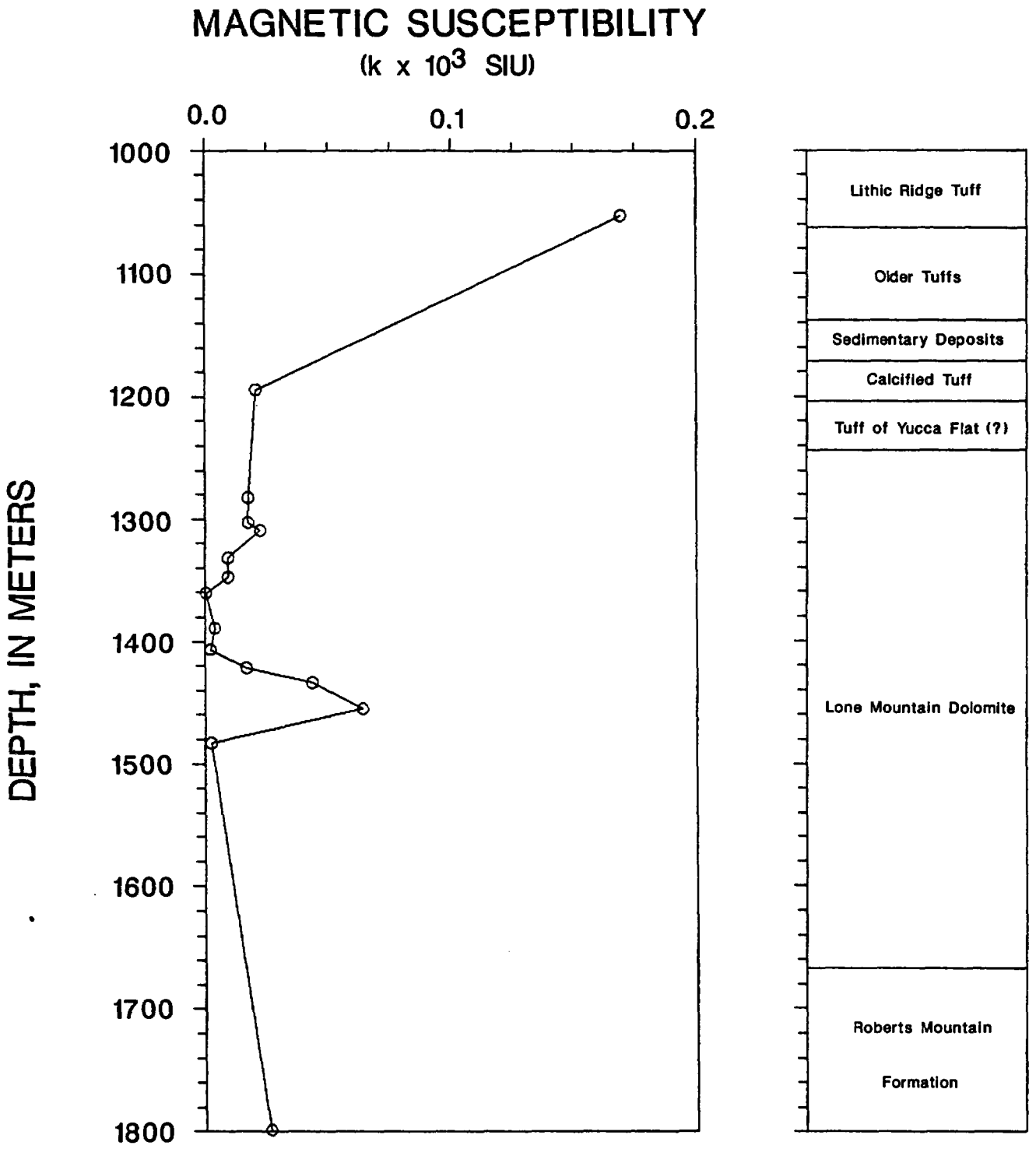

Figure 18. Plot of magnetic susceptibility values measured on core samples from the UE25p#1 borehole.

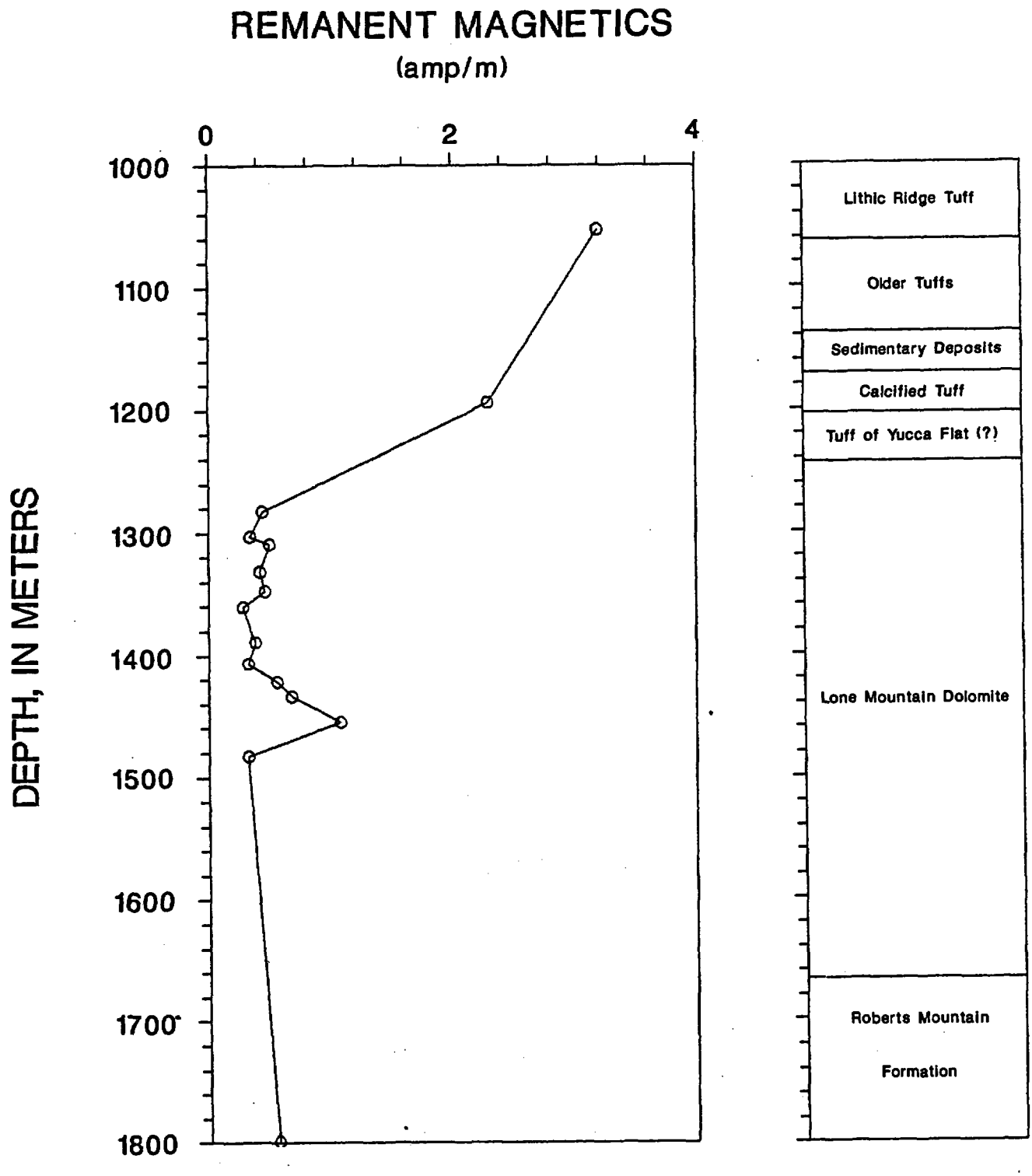

Figure 19. Plot of remanent magnetization values measured on core samples from the UE25p#1 borehole.

Summary

Thirteen of the sixteen samples selected from the lower part of the UE25p#1 borehole were from the Lone Mountain Dolomite so as to establish recognition patterns for that formation when interpreting borehole and surface geophysical data. At the site of the borehole, the Lone Mountain Dolomite forms the break between the Paleozoic rock and the overlying Tertiary units of the Yucca Mountain series. The dolomite is a fine-to-medium-grained crystalline rock containing brecciated intervals. Secondary dolomite forms the matrix within the brecciated zones creating a porosity of about four percent which is low relative to the approximate seventeen percent porosity measured on the Lithic Ridge and Calcified Tuffs. Porosity variations within the Lone Mountain Dolomite, a function of the amount of secondary dolomite contained within the sample, is generally responsible for corresponding variations in the bulk density, sonic velocity, and to some extent, the resistivity of the rock. Grain density measurements indicate the dolomite to be compositionally uniform.

Permeability, in both the vertical and horizontal sense, varied from .0003 to 164 millidarcies; the highest values occurring within the intensely brecciated samples. Fractures filled with either crystallized dolomite or calcite appear to be sufficiently healed to effectively impede the movement of ground water flow.

The dolomites are distinguished by their general lack of magnetic mineral content. As a result the magnetic intensities are only a small fraction of that of the Yucca Mountain tuffs and, as a result, would be expected to contribute little to any local field disturbance.

Rock property data from the single Roberts Mountain sample suggests a less fractured, finer grained rock having a porosity of 0.3 percent and a relatively low water permeability of less than .034 millidarcies. Its 13000 ohm-meter resistivity, possibly its most distinguishing characteristic, is approximately 4000 ohm-meters higher than the highest resistivity measured on any of the Lone Mountain Dolomite samples.

References

Anderson, L.A., 1981, Rock property analysis of core samples from the Yucca Mountain UE25a-1 borehole, Nevada Test Site, Nevada: U.S. Geological Survey Open-File Report 81-1338 (NNA.870406.0031).

Anderson, L.A., 1984, Rock Property measurements on large-volume core samples from the Yucca Mountain USW GU-3/G-3 and USW G-4 boreholes, Nevada Test Site, Nevada: U.S. Geological Survey Open-File Report 84-552 (NNA.870323.0195).

Benson, L.V., and McKinley, P.W., 1985, Chemical composition of ground water in the Yucca Mountain area, Nevada, 1971-84: U.S. Geological Survey Open-File Report 85-484 (NNA.890522.0210).

Carr, M.D., Waddell, S.J., Vick, G.S., Stock, J.M., Monsen, S.A., Harris, A.G., Cork, B.W., and Byers, F.M. Jr., 1986, Geology of drill hole UE25p#1: A test hole into pre-Tertiary rocks near Yucca Mountain, southern Nevada: U.S. Geological Survey Open-File Report 86-175 (HQS.880517.2633).

Chleborad, A.F., Powers, P.S., and Farrow, R.A., 1975, A technique for measuring bulk volume of rock materials: Assoc. Eng. Geologists Bulletin., v. 12, no. 4, pp 307-312 (NNA.910212.0106).

Daniels, J.J., Scott, J.H., and Hagstrom, J.T., 1981, Interpretation of geophysical well-log measurements in drillholes UE25a-4, -5, -6, and -7, Yucca Mountain, Nevada Test Site: U.S. Geological Survey Open-File Report 81-389 (HQS.880517.2658).

Hagstrum, J.T., Daniels, J.J., and Scott, J.H., 1980, Analysis of the magnetic susceptibility well log in drill hole UE25a-5, Yucca Mountain, Nevada Test Site: U.S. Geological Survey Open-File Report 80-1263 (HQS.880517.1249).

Johnson, G.R., 1979, Textural Properties, in Hunt, G.R., Johnson G.R., Olhoeft, G.R., Watson D.E., and Watson, K., Initial report of the petrophysics laboratory: U.S. Geological Survey Circular 789, p. 67-74 (NNA.910212.0107).

Obert, Leonard, and Duvall, Wilbur I., 1967, Rock Mechanics and the design of structures in rock: John Wiley and Sons, Inc., New York, London, Sydney, p. 344-350 (NNA.910212.0108).

Olsen R.E., and Daniel D.E., 1981, Measurement of the hydraulic conductivity of fine-grained soils, in Permeability and groundwater contaminant transport, T.F. Zimmie and C.O. Riggs, Eds., American Society for Testing and Materials STP 746, pp. 18-64 (NNA.910212.0109).

Orkild, P.P., 1965, Paintbrush Tuff and Timber Mountain Tuff of Nye County, Nevada, in Changes in stratigraphic nomenclature by the U.S. Geological Survey: U.S. Geological Survey Bulletin 1224-A, p. A44-A51 (HQS.880517.2039).

Senterfit, R.M., Hoover, D.B., and Chornack, M., 1982, Resistivity sounding investigation by the Schlumberger method in the Yucca Mountain and Jackass Flats area, Nevada Test Site, Nevada: U.S. Geological Survey Open-File Report 82-1043 (HQS.880517.2865).

Spengler, R.W., and Rosenbaum, J.G., 1980, Preliminary interpretations of geologic results obtained from boreholes UE25a-4, -5, -6, and -7, Yucca Mountain, Nevada Test Site: U.S. Geological Survey Open-File Report 80-929 (NNA.890823.0106).

*U.S. GOVERNMENT PRINTING OFFICE 1991-0-673-207/50016

The following number is for U.S. Department of Energy OCRWM management purposes only and should not be used when ordering this publication.
NNA.910411.0081